Enriched two dimensional mixed finite element models for linear elasticity with weak stress symmetry

Philippe R. B. Devloo[a], Sônia M. Gomes[b,*], Thiago O. Quinelato[c], Shudan Tian[d]

[a] *FEC-Universidade Estadual de Campinas, Campinas-SP, Brazil*
[b] *IMECC-Universidade Estadual de Campinas, Campinas, SP, Brazil*
[c] *Universidade Federal de Juiz de Fora, Juiz de Fora, MG, Brazil*
[d] *Peking University, Beijing, China*

Abstract

The purpose of this article is to derive and analyze new discrete mixed approximations for linear elasticity problems with weak stress symmetry. These approximations are based on the application of enriched versions of classic Poisson-compatible spaces, for stress and displacement variables, and/or on enriched Stokes-compatible space configurations, for the choice of rotation spaces used to weakly enforce stress symmetry. Accordingly, the stress space has to be adapted to ensure stability. Such enrichment procedures are done via space increments with extra bubble functions, which have their support on a single element (in the case of H^1-conforming approximations) or with vanishing normal components over element edges (in the case of $H(\mathrm{div})$-conforming spaces). The advantage of using bubbles as stabilization corrections relies on the fact that all extra degrees of freedom can be condensed, in a way that the number of equations to be solved and the matrix structure are not affected. Enhanced approximations are observed when using the resulting enriched space configurations, which may have different orders of accuracy for the different variables. A general error analysis is derived in order to identify the contribution of each kind of bubble increment on the accuracy of the variables, individually. The use of enriched Poisson spaces improves the rates of convergence of stress divergence and displacement variables. Stokes enhancement by bubbles contributes to equilibrate the accuracy of weak stress symmetry enforcement with the stress approximation order, reaching the maximum rate given by the normal traces (which are not affected).

Keywords: Mixed finite element formulations, Linear elasticity, Weak stress symmetry, Enhanced accuracy

*Corresponding author - Phone +55 19 35215950
Email addresses: phil@fec.unicamp.br (Philippe R. B. Devloo), soniag@ime.unicamp.br (Sônia M. Gomes), thiago.quinelato@ice.ufjf.br (Thiago O. Quinelato), tianshudan@pku.edu.cn (Shudan Tian)

1. Introduction

Mixed finite element methods have been used for linear elasticity problems since the very beginning of finite element history [19]. Based on the Hellinger-Reissner principle, these methods seek simultaneous approximations for both the stress and the displacement, the variables of primary interest, as as independent unknowns. Instead, if a traditional H^1-conforming formulation is considered only in terms of displacement, with the stress being obtained through a numerical differentiation of the displacement, it is well known that a decrease in stress accuracy occurs. Furthermore, a correctly designed mixed method (i.e. satisfying the equilibrium condition) gives a good modeling of incompressible and nearly incompressible materials, for which standard displacement methods fail.

Conforming finite element mixed methods require the normal component of the stress tensor $\underline{\underline{\sigma}}$ to be continuous along the inter-element boundaries (i.e., $\underline{\underline{\sigma}} \in \mathscr{S} \subset H(\mathrm{div}, \Omega, \mathbb{M})$), but discontinuous approximation spaces $\mathscr{U} \subset L^2(\Omega, \mathbb{R}^2)$ are used for the displacement variable $\underline{u}$. Moreover, for stability, divergence compatibility of this finite element pair and other requirements are necessary. There is a line of research using symmetric tensor spaces $\mathscr{S}$ (cf. e.g. [16, 22, 27] and references therein), but mixed formulations for linear elasticity problems weakly imposing stress symmetry have also been considered by several authors (c.f. e.g. [1, 6, 8, 12, 17, 21, 26, 28]). Both approaches may deliver optimal convergence rates for the stress tensor and displacement, symmetric tensors requiring smaller system of equations when compared to the weakly symmetric approximations. The symmetric tensor approximations, however, lead to lower convergence orders when applied to problems where the elastic coefficients are heterogeneous. Moreover, as mentioned in [2], the stability requirements have proved to be surprisingly hard to be fulfilled by symmetric tensors. For these reasons, other strategies have been pursued, by weakening the enforcement of stress symmetry, the main subject of this article, or by giving up $H(\mathrm{div})$-consistency in the so called non-conforming methods (e.g. [3, 7, 23, 25, 30] and the references therein), which we will not treat here.

For the mixed formulations weakly imposing stress symmetry, in addition to divergence compatible approximation spaces $\mathscr{S} \subset H(\mathrm{div}, \Omega, \mathbb{M})$, and $\mathscr{U} \subset L^2(\Omega, \mathbb{R}^2)$, for stress and displacement variables, the idea consists in imposing a weak symmetry condition through the use of a Lagrange multiplier living in an appropriate approximation space $\mathscr{Q}$. Usually, the spaces $\{\mathscr{S}, \mathscr{U}\}$ are obtained with rows taken from a compatible space configuration $\{\mathscr{V}, \mathscr{P}\}$ for the mixed formulation of Poisson problems, based on a partition $\mathcal{T} = \{K\}$ of the computational domain Ω. For stability, the multiplier space $\mathscr{Q}$ should be chosen properly. For two dimensional problems, one methodology for stability analysis consists in finding a Stokes-compatible space configuration $\{\mathscr{W}, \mathscr{Q}\}$, for velocity and pressure variables. If $\mathscr{S}$ contains the curl of $\mathscr{W}$, then $\{\mathscr{S}, \mathscr{U}, \mathscr{Q}\}$ can be stably applied to the mixed formulation for elasticity with weak stress symmetry.

Given a stable space configuration $\{\mathscr{S}, \mathscr{U}, \mathscr{Q}\}$, our purpose is to obtain new methods by enriching the spaces $\mathscr{U}$, $\mathscr{Q}$, or both. Consequently, the stress space has also to be adapted to restore stability. For such kind of space configurations, with enhanced and possibly different

rates of convergence for the different variables, a general error analysis is derived in Section 4, for which the error for each variable is estimated individually, in terms of projection errors. As indicated in the proofs, the theoretical analysis combines some classic tools previously used by other authors. However, for stability, two new auxiliary types of Stokes-compatible space configurations were created.

The enrichment procedures shall be enforced by space increments using extra bubble terms. Bubbles refer to functions with support on a single element (in the case of H^1-conforming approximations) or with vanishing normal components over element edges (in the case of $H(\mathrm{div})$-conforming spaces). The advantage of using bubbles as stabilization corrections relies on the fact that the corresponding degrees of freedom can all be condensed, in a way that the number of equations to be solved and the matrix structure are not affected by the enrichment process.

One kind of enrichment consists in taking a higher order rotation space $\mathscr{Q}^+ \supset \mathscr{Q}$, requiring a richer Stokes-compatible configuration $\{\mathscr{W}^+, \mathscr{Q}^+\}$ for the corresponding stability analysis. As described in [11], stabilization of approximation spaces for Stokes problems using a richer pressure space $\mathscr{Q}^+$ can be obtained by the addition of some proper bubble functions to form $\mathscr{W}^+$. Thus, the effect of this procedure on the elasticity space configuration is an increment of $\mathscr{S}$ by higher order divergence-free bubble functions to form $\mathscr{S}^+$, without changing $\mathscr{U}$. One example in this context is discussed by Stenberg in [28], based on the Poisson-compatible $\mathcal{BDM}_k$ spaces for triangles, which can be viewed as an enriched version of the Arnold-Falk-Winther family [6] by the increment of the tensor spaces by divergence-free bubbles in order to enhance the multiplier space (see Section 6.3). As illustrated in Section 5, and having in mind the design of stable space configurations for elasticity problems with higher order multiplier spaces, two new richer Stokes-compatible space configurations shall be created, namely $\mathcal{CR}_k^+$ for triangular elements, corresponding to an enriched version of the Crouzeix-Raviart space $\mathcal{CR}_k$, for $k = 2, 3$ [13], extended for higher orders in [24], and $\mathcal{GR}_{[k]}^+$ for quadrilateral meshes, an enriched version of the Girault-Raviart ($\mathcal{GR}_{[k]}$) space [20], for $k \geq 1$.

There are other circumstances where the goal is to have richer displacement approximations $\mathscr{U}^+ \supset \mathscr{U}$. Assuming that the pair $\{\mathscr{S}, \mathscr{U}\}$ is constructed from a Poisson-compatible space configuration $\{\mathscr{V}, \mathscr{P}\}$, it seems natural to take an enriched stable version $\{\mathscr{V}^+, \mathscr{P}^+\}$ to form $\{\mathscr{S}^+, \mathscr{U}^+, \mathscr{Q}\}$. For such cases, the same Stokes-compatible space configuration $\{\mathscr{W}, \mathscr{Q}\}$ used for the stability analysis of the original space configuration $\{\mathscr{S}, \mathscr{U}, \mathscr{Q}\}$ can be used to prove stability for the enriched version $\{\mathscr{S}^+, \mathscr{U}^+, \mathscr{Q}\}$. For instance, this is the case of space configuration based on Poisson-compatible $\mathcal{ABF}_{[k]}$ spaces for quadrilateral meshes, discussed in [26], which can be viewed as an enriched version of the family based on $\mathcal{RT}_{[k]}$ spaces discussed in [1]. The adoption of enriched $\mathcal{ABF}_{[k]}$ spaces enhances the accuracy of stress divergence and displacement, but it is not sufficient to improve the weak enforcement of stress symmetry in general quadrilateral meshes.

As proposed in [18, 14], there are other enriched stable spaces $\{\mathscr{V}^+, \mathscr{P}^+\}$ for the Poisson problem that can be obtained by adding to $\mathscr{V}$ some appropriate bubble functions to form $\mathscr{V}^+$, keeping unchanged the original edge vector functions. Some examples shall be considered

in Section 5, as well as their corresponding enriched versions, which are used in the current study. The corresponding stable finite element spaces $\mathscr{S} \subset H(\mathrm{div}, \Omega, \mathbb{M}), \mathscr{U} \subset L^2(\Omega, \mathbb{R}^2)$, $\mathscr{Q} \subset L^2(\Omega, \mathbb{R})$ for the mixed method for linear elasticity with weakly imposed stress symmetry are listed in Table 1, where the associated local spaces $S(K, \mathbb{M})$, $U(K, \mathbb{R}^2)$, and $Q(K, \mathbb{R})$ are shown.

As shall be discussed in Section 6, the effect of using these kinds of enriched Poisson-compatible spaces to form displacement and stress approximations for linear elasticity enhances the divergence and displacement variables. Since weak stress symmetry enforcement and stress accuracy result to be related, space enrichment can be used to equilibrate them, reaching the maximum rate given by the order of stress normal traces, which are not affected (see Table 3).

Geometry	P-method	S	U	Q	Reference
Triangular	$\mathcal{BDM}_k$	$\mathbb{P}_k$	$\mathbb{P}_{k-1}$	$\mathbb{P}_{k-1}$	[6]
	$\mathcal{BDM}_k^+$	$\mathbb{P}_k^\partial \oplus \mathring{\mathbb{P}}_{k+1}$	$\mathbb{P}_k$	$\mathbb{P}_k$	this paper[1]
	$\mathcal{BDM}_k^{++}$	$\mathbb{P}_k^\partial \oplus \mathring{\mathbb{P}}_{k+2}$	$\mathbb{P}_{k+1}$	$\mathbb{P}_{k+1}$	this paper
Quadrilateral	$\mathcal{RT}_{[k]}$	$V_{\mathcal{RT}_{[k]}}$	$P_{\mathcal{RT}_{[k]}}$	$\mathbb{P}_k$	[1]
	$\mathcal{RT}_{[k]}^+$	$V_{\mathcal{RT}_{[k]}}^\partial \oplus \mathring{V}_{\mathcal{RT}_{[k+1]}}$	$P_{\mathcal{RT}_{[k+1]}}$	$\mathbb{P}_{k+1}$	this paper

Table 1: The discussed and implemented combinations of stable finite element spaces $\mathscr{S} \subset H(\mathrm{div}, \Omega, \mathbb{M}), \mathscr{U} \subset L^2(\Omega, \mathbb{R}^2)$, $\mathscr{Q} \subset L^2(\Omega, \mathbb{R})$ for the mixed approximation of linear elasticity with weakly imposed stress symmetry, with corresponding local spaces S, U and Q, constructed from Poisson-compatible methods (P-method) for triangular and quadrilateral meshes.

The paper is organized as follows. General aspects on notation for element geometry, polynomial spaces, differential operators, transformations, and approximation spaces are set in Section 2. The mixed element formulation for linear elasticity problems with weak stress symmetry is given in Section 3, for which a general error analysis script is established in Section 4. The required Poisson-compatible and Stokes compatible space configurations, and their enriched versions, are discussed in Section 5. The proposed enhanced approximation space configurations for the mixed formulation for linear elasticity problems with weak enforcement of stress symmetry are described in Section 6, where convergence rates are determined by identifying the principal hypotheses required by the general script of Section 4. Section 7 contains some numerical results illustrating the theoretical a priori estimates of previous sections.

2. Preliminaries

We begin by collecting some useful notation and fundamental aspects of compatible approximation spaces for Poisson and Stokes problems with which we explain the analysis of the methods proposed in the paper.

[1] It can be shown that this space is equivalent to the one proposed in [28]. In this paper we construct it by the composition of edge and internal functions (see Section 6.3.1).

2.1. Notation for vector and tensor functional spaces

We use $\mathbb{M} = \mathbb{R}^{2\times 2}$ to refer to the space of two-dimensional second-order tensors, while $\mathbb{S} \subset \mathbb{M}$ is the subspace of symmetric tensors. Scalar functional Hilbert spaces $L^2(\Omega, \mathbb{R})$ and $H^s(\Omega, \mathbb{R})$ have the usual meaning and norms. Associated vector and tensor spaces inherit the corresponding norms, and shall be denoted by:

$$
\begin{aligned}
L^2(\Omega, \mathbb{R}^2) &= [L^2(\Omega, \mathbb{R})]^2;\ H^s(\Omega, \mathbb{R}^2) = [H^s(\Omega, \mathbb{R})]^2. \\
L^2(\Omega, \mathbb{M}) &= [L^2(\Omega, \mathbb{R})]^{2\times 2};\ H^s(\Omega, \mathbb{M}) = [H^s(\Omega, \mathbb{R})]^{2\times 2}. \\
H(\mathrm{div}, \Omega, \mathbb{R}^2) &= \left\{ \underline{q} \in L^2(\Omega, \mathbb{R}^2);\ \nabla \cdot \underline{q} \in L^2(\Omega, \mathbb{R}) \right\}. \\
H(\mathrm{div}, \Omega, \mathbb{M}) &= \left\{ \underline{\underline{q}} \in L^2(\Omega, \mathbb{M});\ \underline{\nabla} \cdot \underline{\underline{q}} \in L^2(\Omega, \mathbb{R}^2) \right\}.
\end{aligned}
$$

Throughout the text, $(\ ,\ )$ denotes inner products in $L^2(\Omega, \mathbb{R})$, $L^2(\Omega, \mathbb{R}^2)$, and $L^2(\Omega, \mathbb{M})$, and $\langle\ ,\ \rangle$ is used to define the duality pairing between $H^{-1/2}(\partial\Omega, \mathbb{R}^2)$, the space of normal traces of $H(\mathrm{div}, \Omega, \mathbb{M})$, and $H^{1/2}(\partial\Omega, \mathbb{R}^2)$, the space of traces of $H^1(\Omega, \mathbb{R}^2)$.

2.2. Operators

- *Divergence* ($\nabla \cdot$ and $\underline{\nabla}\cdot$):
  For a vector function $\underline{q} = [\psi_1\ \psi_2]^T$, $\nabla \cdot \underline{q} = \partial_1\psi_1 + \partial_2\psi_2$;
  For a tensor function $\underline{\underline{q}} = \begin{bmatrix} \psi_{11} & \psi_{12} \\ \psi_{21} & \psi_{22} \end{bmatrix} = \begin{bmatrix} \underline{\psi}_1 \\ \underline{\psi}_2 \end{bmatrix}$, $\underline{\nabla} \cdot \underline{\underline{q}} = \begin{bmatrix} \nabla \cdot \underline{\psi}_1 \\ \nabla \cdot \underline{\psi}_2 \end{bmatrix}$.
- *Curl* ($\underline{\nabla} \times$ and $\underline{\underline{\nabla}}\times$):
  For a scalar function ψ, $\underline{\nabla} \times \psi = \begin{bmatrix} \partial_2\psi & -\partial_1\psi \end{bmatrix}$;
  For a vector function $\underline{q} = \begin{bmatrix} q_1 \\ q_2 \end{bmatrix}$, $\underline{\underline{\nabla}} \times \underline{q} = \begin{bmatrix} \underline{\nabla} \times q_1 \\ \underline{\nabla} \times q_2 \end{bmatrix} = \begin{bmatrix} \partial_2 q_1 & -\partial_1 q_1 \\ \partial_2 q_2 & -\partial_1 q_2 \end{bmatrix}$;
  For the product of scalar and vector functions $\psi\underline{q}$: $\underline{\underline{\nabla}} \times (\psi\underline{q}) = \psi\underline{\underline{\nabla}} \times \underline{q} + \underline{q}\underline{\nabla} \times \psi$.
- *Asymmetry measure* (asym):
  For $\underline{\underline{q}} = \begin{bmatrix} \psi_{11} & \psi_{12} \\ \psi_{21} & \psi_{22} \end{bmatrix}$, $\mathrm{asym}\,\underline{\underline{q}} = \psi_{12} - \psi_{21}$;
  $\mathrm{asym} : H(\mathrm{div}, \Omega, \mathbb{M}) \to L^2(\Omega, \mathbb{R})$ is a bounded operator.

2.3. Local approximation spaces restricted to an element K

Scalar spaces:

- $\mathbb{P}_k(K, \mathbb{R})$ - scalar polynomials of total degree at most k;
- $\mathbb{Q}_{k,t}(K, \mathbb{R})$ - scalar polynomials of maximum degree k in x and t in y;
- $\tilde{\mathbb{P}}_k(K, \mathbb{R})$ - homogeneous polynomials of degree k.

Vector spaces $V(K,\mathbb{R}^2) = V^{\partial}(K,\mathbb{R}^2) \oplus \mathring{V}(K,\mathbb{R}^2)$

- $V^{\partial}(K,\mathbb{R}^2)$ - edge functions;
- $\mathring{V}(K,\mathbb{R}^2)$ - internal functions.

Tensor spaces $S(K,\mathbb{M})$

- Rows in $S(K,\mathbb{M})$ are vectors in $V(K,\mathbb{R}^2)$.

2.4. Transformations

Let $F_K : \hat{K} \to K$ be a geometric invertible map transforming $\hat{K}$ onto K. $F_K : \hat{K} \to K$ is supposed to be affine $F_K(\hat{x},\hat{y}) = \mathbf{A}_0 + \mathbf{A}_1\hat{x} + \mathbf{A}_2\hat{y}$ (triangles and parallelograms), or non-affine $F_K(\hat{x},\hat{y}) = \mathbf{A}_0 + \mathbf{A}_1\hat{x} + \mathbf{A}_2\hat{y} + \mathbf{A}_3\hat{x}\hat{y}$ (non-parallelogram quadrilaterals).

- Scalar functions: $p = \mathbb{F}_K\hat{p} = \hat{p} \circ F_K^{-1}$; for vector functions $\underline{q} = \mathbb{F}_K\underline{\hat{q}}$ by applying $\mathbb{F}_K$ to the components of $\underline{\hat{q}}$;
- Vector functions (Piola transformation): $\underline{q} = \mathbb{F}_K^{\mathrm{div}}\underline{\hat{q}} = \mathbb{F}_K\left[\dfrac{1}{\mathbf{J}_K}\,\mathrm{D}F_K\underline{\hat{q}}\right]$, where $\mathrm{D}F_K$ is the Jacobian matrix of F_K, and $\mathbf{J}_K = \left|\det(\mathrm{D}F_K)\right|$;
- For tensors: $\underline{\underline{q}} = \mathbb{F}_K^{\mathrm{div}}\underline{\underline{\hat{q}}}$ is defined by applying the Piola transformation to each row of $\underline{\underline{\hat{q}}}$.

Properties [1, Lemma 2]

1. $\nabla \cdot \underline{q} = \mathbb{F}_K\left[\dfrac{1}{\mathbf{J}_K}\,\nabla\cdot\underline{\hat{q}}\right]$.
2. For vector functions $\underline{q} = \mathbb{F}_K\underline{\hat{q}}$, $\underline{\nabla} \times \underline{q} = \mathbb{F}_K^{\mathrm{div}}\underline{\nabla} \times \underline{\hat{q}}$.

2.5. Poisson-compatible approximation spaces

Approximations spaces for flux $\mathscr{V} \subset H(\mathrm{div},\Omega,\mathbb{R}^2)$ and pressure $\mathscr{P} \subset L^2(\Omega,\mathbb{R})$, to be used in the mixed formulation of Poisson problems, are generally piecewise defined as

$$\mathscr{V} = \left\{\underline{\eta} \in H(\mathrm{div},\Omega,\mathbb{R}^2);\ \underline{\eta}|_K \in V(K,\mathbb{R}^2),\ K \in \mathcal{T}\right\}, \tag{1}$$

$$\mathscr{P} = \left\{p \in L^2(\Omega,\mathbb{R});\ p|_K \in P(K,\mathbb{R}),\ K \in \mathcal{T}\right\}. \tag{2}$$

The local spaces $V(K,\mathbb{R}^2) \subset H(\mathrm{div},K,\mathbb{R}^2)$ and $P(K,\mathbb{R}) \subset L^2(K,\mathbb{R})$ can be defined directly on the geometric element K, or by backtracking a vector polynomial space $\hat{\mathbf{V}}$ and a scalar polynomial space $\hat{P}$, which are defined on a reference element $\hat{K}$. Precisely, if $F_K : \hat{K} \to K$ is the geometric transformation of $\hat{K}$ onto K, then $P(K,\mathbb{R}) = \mathbb{F}_K\hat{P}$, and $V(K,\mathbb{R}^2) = \mathbb{F}_K^{\mathrm{div}}\hat{\mathbf{V}}$.

For compatibility, the following condition is required:

$$\nabla \cdot \hat{\mathbf{V}} = \hat{P}. \tag{3}$$

In this paper we consider that $\hat{\mathbf{V}}$ is spanned by a hierarchy of vector shape functions organized into two classes: the functions of interior type, with vanishing normal components over

all element edges, $\mathring{\hat{\mathbf{V}}}$, and the shape functions associated to the element edges $\hat{\mathbf{V}}^{\partial}$. Thus, the decomposition $\hat{\mathbf{V}} = \mathring{\hat{\mathbf{V}}} \oplus \hat{\mathbf{V}}^{\partial}$ naturally holds.

Property (3) can be extended to the spaces $\mathscr{V}$ and $\mathscr{P}$. Precisely, let $\hat{\lambda}$ be the L^2-orthogonal projection on $\hat{P}$, and let $\hat{\boldsymbol{\pi}} : H^s(\hat{K}, \mathbb{R}^2) \to \hat{\mathbf{V}}$ be an appropriate projection commuting the de Rham diagram

$$\nabla \cdot (\hat{\boldsymbol{\pi}} \hat{\underline{\eta}}) = \hat{\lambda}(\nabla \cdot \hat{\underline{\eta}}).$$

Analogously, on the geometric element K, define $\lambda_K : L^2(K, \mathbb{R}) \to P(K, \mathbb{R})$ by $\lambda_K(p) = \hat{\lambda}(\hat{p}) \circ \mathbb{F}_K^{-1}$, with $\hat{p} = p \circ \mathbb{F}_K$. Then $\lambda : L^2(\Omega, \mathbb{R}) \to \mathscr{P}$ is defined by $\lambda(p)|_K = \lambda_K(p|_K)$. Analogously, projection $\boldsymbol{\pi}^D : H^s(\Omega, \mathbb{R}^2) \to \mathscr{V}$ is defined in terms of local projections $\boldsymbol{\pi}_K : H^s(K, \mathbb{R}^2) \to V(K, \mathbb{R}^2)$, where $\boldsymbol{\pi}_K(\underline{\eta}) = \hat{\boldsymbol{\pi}}(\hat{\underline{\eta}}) \circ \mathbb{F}_K^{-1}$, with $\hat{\underline{\eta}} = \underline{\eta} \circ \mathbb{F}_K^{\mathrm{div}}$. It follows that

$$(p - \lambda p, \nabla \cdot \underline{q}) = 0, \quad \forall \underline{q} \in \mathscr{V}, \tag{4a}$$

$$(\nabla \cdot (\underline{\eta} - \boldsymbol{\pi}^D \underline{\eta}), \psi) = 0, \quad \forall \psi \in \mathscr{P}. \tag{4b}$$

2.6. Stokes-compatible approximation spaces

Stokes-compatible approximations $\mathscr{W} \subset H^1(\Omega, \mathbb{R}^2)$ for velocity, and $\mathscr{Q} \subset L^2(\Omega, \mathbb{R})$ for pressure, to be used in a mixed formulation for Stokes problems, are generally piecewise defined as

$$\mathscr{W} = \left\{ \underline{w} \in H^1(\Omega, \mathbb{R}^2);\ \underline{w}|_K \in W(K, \mathbb{R}^2),\ K \in \mathcal{T} \right\},$$
$$\mathscr{Q} = \left\{ q \in L^2(\Omega, \mathbb{R});\ q|_K \in Q(K, \mathbb{R}),\ K \in \mathcal{T} \right\}.$$

The local spaces can also be defined directly on the geometric element K or by backtracking a vector polynomial space $\hat{\mathbf{W}}$ and a scalar polynomial $\hat{Q}$, which are defined on a reference element $\hat{K}$. Precisely, $W(K, \mathbb{R}^2) = \mathbb{F}_K \hat{\mathbf{W}}$, $Q(K, \mathbb{R}) = \mathbb{F}_K \hat{Q}$.

As discussed in [9], there are cases, specially for general quadrilateral meshes, where the use of *unmapped* pressure spaces $\mathscr{Q}$ are more effective, meaning that $Q(K, \mathbb{R})$ is a polynomial space defined directly in K.

For stability, the well known inf-sup condition should be verified:

- There exists a positive constant C such that for each $q \in \mathscr{Q}$ there is a nonzero $\underline{w} \in \mathscr{W}$ with $(\nabla \cdot \underline{w}, q) \geq C \|\underline{w}\|_{H^1} \|q\|_{L2}$.

The inf-sup condition holds provided a bounded linear operator $\boldsymbol{\pi}^S : H^s(\Omega, \mathbb{R}^2) \to \mathscr{W}$ exists verifying:

$$\left(\nabla \cdot (\underline{w} - \boldsymbol{\pi}^S \underline{w}), \psi \right) = 0,\ \forall \psi \in \mathscr{Q}.$$

3. Mixed formulation for elasticity problems with weak stress symmetry

Consider the mixed formulation with weak stress symmetry for the elasticity problem: Given $\underline{u}_D \in H^{\frac{1}{2}}(\partial\Omega, \mathbb{R}^2)$ and $\underline{g} \in L^2(\Omega, \mathbb{R}^2)$, find $(\underline{\sigma}, \underline{u}, q) \in H(\mathrm{div}, \Omega, \mathbb{M}) \times L^2(\Omega, \mathbb{R}^2) \times L^2(\Omega, \mathbb{R})$

satisfying

$$(\mathbf{A}\underline{\underline{\sigma}}, \underline{\underline{\tau}}) + (\underline{u}, \underline{\nabla} \cdot \underline{\underline{\tau}}) + (q, \operatorname{asym} \underline{\underline{\tau}}) = \langle \underline{\underline{\tau}}\underline{\nu}, \underline{u}_D \rangle, \quad \forall \underline{\underline{\tau}} \in H(\operatorname{div}, \Omega, \mathbb{M}), \tag{5a}$$

$$(\underline{\nabla} \cdot \underline{\underline{\sigma}}, \underline{\eta}) = (\underline{g}, \underline{\eta}), \qquad \forall \underline{\eta} \in L^2(\Omega, \mathbb{R}^2), \tag{5b}$$

$$(\operatorname{asym} \underline{\underline{\sigma}}, \varphi) = 0, \qquad \forall \varphi \in L^2(\Omega, \mathbb{R}), \tag{5c}$$

for the stress tensor $\underline{\underline{\sigma}}$, the displacement $\underline{u}$, and the rotation $q = \operatorname{asym}(\nabla \underline{u}/2)$. The material properties are described by a compliance tensor $\mathbf{A} = \mathbf{A}(\mathbf{x})$, which is a self-adjoint, bounded, and uniformly positive definite linear operator acting from $\mathbb{S}$ to $\mathbb{S}$. We assume that $\mathbf{A}$ can be extended to an operator from $\mathbb{M}$ to $\mathbb{M}$ with the same properties. In particular, in the case of homogeneous and isotropic body, $\mathbf{A}\underline{\underline{\varepsilon}} = 2\mu\underline{\underline{\varepsilon}} + \lambda \operatorname{tr}(\underline{\underline{\varepsilon}})\underline{\underline{I}}$, λ and μ being the Lamé parameters, and $\underline{\underline{I}}$ the 2×2 identity matrix. Throughout this paper, the variables shall be assumed to be normalized, such that this formulation is dimensionless.

Remark

A more general way of presenting this formulation would be to define the rotation as an anti-symmetric tensor. This idea generalizes to the three-dimensional case and was the choice of many authors, e.g., [6, 12].

Discrete formulation

Given finite dimensional subspaces $\mathscr{S} \subset H(\operatorname{div}, \Omega, \mathbb{M})$ for tensors, $\mathscr{U} \subset L^2(\Omega, \mathbb{R}^2)$ for displacements, and $\mathscr{Q} \subset L^2(\Omega, \mathbb{R})$ for rotations, consider the discrete version of the formulation: find $(\underline{\underline{\sigma}}, \underline{u}, q) \in \mathscr{S} \times \mathscr{U} \times \mathscr{Q}$ satisfying

$$(\mathbf{A}\underline{\underline{\sigma}}, \underline{\underline{\tau}}) + (\underline{u}, \underline{\nabla} \cdot \underline{\underline{\tau}}) + (q, \operatorname{asym} \underline{\underline{\tau}}) = \langle \underline{\underline{\tau}}\underline{\nu}, \underline{u}_D \rangle, \quad \forall \underline{\underline{\tau}} \in \mathscr{S}, \tag{6a}$$

$$(\underline{\nabla} \cdot \underline{\underline{\sigma}}, \underline{\eta}) = (\underline{g}, \underline{\eta}), \qquad \forall \underline{\eta} \in \mathscr{U}, \tag{6b}$$

$$(\operatorname{asym} \underline{\underline{\sigma}}, \varphi) = 0, \qquad \forall \varphi \in \mathscr{Q}. \tag{6c}$$

Stability

The inf-sup condition for this formulation holds provided the following Brezzi's stability conditions are satisfied:

(S1) There exists a positive constant c_1 such that $\|\underline{\underline{\tau}}\|_{H(\operatorname{div},\Omega,\mathbb{M})} \leq c_1(\mathbf{A}\underline{\underline{\tau}}, \underline{\underline{\tau}})^{1/2}$ whenever $\underline{\underline{\tau}} \in \mathscr{S}$ satisfies $(\underline{\nabla} \cdot \underline{\underline{\tau}}, \underline{\eta}) = 0$ for all $\underline{\eta} \in \mathscr{U}$, and $(\operatorname{asym}\ \underline{\underline{\tau}}, \varphi) = 0$ for all $\varphi \in \mathscr{Q}$.

(S2) There exists a positive constant c_2 such that for each $\underline{\eta} \in \mathscr{U}$ and $\varphi \in \mathscr{Q}$ there is a nonzero $\underline{\underline{\tau}} \in \mathscr{S}$ with

$$(\underline{\nabla} \cdot \underline{\underline{\tau}}, \underline{\eta}) + (\operatorname{asym}\ \underline{\underline{\tau}}, \varphi) \geq c_2 \|\underline{\underline{\tau}}\|_{H(\operatorname{div},\Omega,\mathbb{M})} (\|\underline{\eta}\|_{L^2(\Omega,\mathbb{R}^2)} + \|\varphi\|_{L^2(\Omega,\mathbb{R})}).$$

One technique to construct stable space configurations for the mixed formulation for elasticity problems with weak symmetry, using Poisson-compatible approximations, is based on

Stokes-compatible spaces, as originally proposed in [17], and stated in the next theorem (see also [8, Proposition 3], [12, Proposition 5.1], [1, Theorem 1]).

Theorem 1. *Let $\mathscr{V} \subset H(\mathrm{div}, \Omega, \mathbb{R}^2)$ and $\mathscr{P} \subset L^2(\Omega, \mathbb{R})$ be a consistent pair of approximation spaces for the mixed formulation of the Poisson problem, and let $\mathscr{W} \subset H^1(\Omega, \mathbb{R}^2)$ and $\mathscr{Q} \subset L^2(\Omega, \mathbb{R})$ be a consistent pair of approximation spaces for the Stokes problem. If*

$$\underline{\underline{\nabla}} \times \mathscr{W} \subset \mathscr{S}, \tag{7}$$

then the space configuration $\mathscr{S} \subset H(\mathrm{div}, \Omega, \mathbb{M})$, with rows in $\mathscr{V}$, $\mathscr{U} \subset L^2(\Omega, \mathbb{R}^2)$, with components in $\mathscr{P}$, and $\mathscr{Q} \subset L^2(\Omega, \mathbb{R})$ satisfies the Brezzi's conditions for the mixed weakly symmetric formulation.

3.1. Approximation spaces

Based on Theorem 1, all formulations to be studied here shall be based on space configurations of the form $\{\mathscr{S}, \mathscr{U}, \mathscr{Q}\}$, where

$$\mathscr{S} = \left\{ \underline{\underline{\tau}} \in H(\mathrm{div}, \Omega, \mathbb{M});\ \underline{\underline{\tau}}|_K \in S(K, \mathbb{M}),\ \forall K \in \mathcal{T} \right\}, \tag{8}$$

$$\mathscr{U} = \left\{ \underline{u} \in L^2(\Omega, \mathbb{R}^2);\ \underline{u}|_K \in U(K, \mathbb{R}^2),\ \forall K \in \mathcal{T} \right\}, \tag{9}$$

$$\mathscr{Q} = \left\{ q \in L^2(\Omega, \mathbb{R});\ q|_K \in Q(K, \mathbb{R}),\ \forall K \in \mathcal{T} \right\} \tag{10}$$

are defined in terms of Poisson-compatible approximation spaces $\mathscr{V} \subset H(\mathrm{div}, \Omega, \mathbb{R}^2)$ and $\mathscr{P} \subset L^2(\Omega, \mathbb{R})$, as in (1) and (2), and $\mathscr{Q} \subset L^2(\Omega, \mathbb{R})$ is the pressure approximation space for a Stokes-compatible space configuration $\{\mathscr{W}, \mathscr{Q}\}$, such that (7) is satisfied. Recall that the local approximation spaces $S(K, \mathbb{M})$ and $U(K, \mathbb{R}^2)$ are constructed in such a way that the rows in $S(K, \mathbb{M})$ are the vectors in $V(K, \mathbb{R}^2)$ and the components of $U(K, \mathbb{R}^2)$ are in $P(K, \mathbb{R})$. When $V(K, \mathbb{R}^2) = V_{\mathrm{NAME}}(K, \mathbb{R}^2)$ and $P(K, \mathbb{R}) = P_{\mathrm{NAME}}(K, \mathbb{R})$ correspond to the local spaces of the family "NAME" for approximation of the Poisson problem, then the equivalent stress and displacement spaces are denoted by $S_{\mathrm{NAME}}(K, \mathbb{M})$ and $U_{\mathrm{NAME}}(K, \mathbb{R}^2)$.

3.2. Projections

Error analyses of approximated mixed methods require the estimation of the best approximation allowed by the spaces, which are usually bounded in terms of some special projection errors. For the mixed formulation of elasticity problems with weak symmetry, appropriate projections are defined in [8], as stated in the next theorem. For completion, the proof is included in Appendix A.

Theorem 2. *Assume compatible approximation spaces $\mathscr{S} \subset H(\mathrm{div}, \Omega, \mathbb{M})$, $\mathscr{U} \subset L^2(\Omega, \mathbb{R}^2)$, and $\mathscr{Q} \subset L^2(\Omega, \mathbb{R})$, as defined in (8), (9), and (10), constructed using the procedure described in Theorem 1. Then, a bounded projection operator $\boldsymbol{\Pi} : H^s(\Omega, \mathbb{M}) \to \mathscr{S}$ can be defined for sufficiently smooth tensors $\underline{\underline{\tau}}$ such that*

$$\left(\underline{\nabla} \cdot (\underline{\underline{\tau}} - \boldsymbol{\Pi}\underline{\underline{\tau}}), \underline{\eta} \right) + \left(\mathrm{asym}(\underline{\underline{\tau}} - \boldsymbol{\Pi}\underline{\underline{\tau}}), \varphi \right) = 0,\ \forall \underline{\eta} \in \mathscr{U},\ \varphi \in \mathscr{Q}. \tag{11}$$

Projection errors

Consider a family a shape-regular partitions $\mathcal{T}_h$, with mesh width h. Let $\mathscr{V}_h$ and $\mathscr{P}_h$ be stable pairs of spaces for the Poisson problem, and let $\boldsymbol{\pi}_h^D$ and λ_h be the associated compatible projections. According to [5, Theorems 4.1 and 4.2], and [4, Theorem 3], projection error estimates

$$\|\underline{\beta} - \boldsymbol{\pi}_h^D \underline{\beta}\|_{L^2(\Omega,\mathbb{R}^2)} \leq Ch^{s+1} \|\underline{\beta}\|_{H^{s+1}(\Omega,\mathbb{R}^2)}, \tag{12}$$

$$\|\nabla \cdot \underline{\beta} - \nabla \cdot \boldsymbol{\pi}_h^D \underline{\beta}\|_{L^2(\Omega,\mathbb{R})} \leq Ch^{l+1} \|\nabla \cdot \underline{\beta}\|_{H^{l+1}(\Omega,\mathbb{R})}, \tag{13}$$

$$\|p - \lambda_h p\|_{L^2(\Omega,\mathbb{R})} \leq Ch^{t+1} \|p\|_{H^{t+1}(\Omega,\mathbb{R})}, \tag{14}$$

hold provided that $\mathbb{P}_s(K,\mathbb{R}^2) \subset V(K,\mathbb{R}^2)$, $\mathbb{P}_l(K,\mathbb{R}) \subset \nabla \cdot V(K,\mathbb{R}^2)$, and $\mathbb{P}_t(K,\mathbb{R}) \subset P(K,\mathbb{R})$.

Accordingly, consider compatible approximation spaces for the elasticity problem: $\mathscr{S}_h \subset H(\mathrm{div},\Omega,\mathbb{M})$, with rows in $\mathscr{V}_h$, $\mathscr{U}_h \subset L^2(\Omega,\mathbb{R}^2)$, with components in $\mathscr{P}_h$, and $\mathscr{Q}_h \subset L^2(\Omega,\mathbb{R})$, as stated in Theorem 1. Let $\boldsymbol{\Pi}_h = \boldsymbol{\Pi}_{1h} + \boldsymbol{\Pi}_{2h}$ be projections $\boldsymbol{\Pi}_h : H^s(\Omega,\mathbb{M}) \to \mathscr{S}_h$ as described in Appendix A. Recall that $\|\boldsymbol{\Pi}_{2h}\underline{\underline{\sigma}}\|_{L^2(\Omega,\mathbb{M})} \leq C\|\underline{\underline{\sigma}} - \boldsymbol{\Pi}_{1h}\underline{\underline{\sigma}}\|_{L^2(\Omega,\mathbb{M})}$, and that $\underline{\nabla} \cdot \boldsymbol{\Pi}_{2h}\underline{\underline{\sigma}} = \underline{0}$. Furthermore, consider $\Lambda_h : L^2(\Omega,\mathbb{R}^2) \to \mathscr{U}_h$ the associated projection $\Lambda_h \underline{u} = [\lambda_h u_1 \ \lambda_h u_2]^T$, for $\underline{u} = [u_1 \ u_2]^T$, so that

$$(\underline{u} - \Lambda_h(\underline{u}), \nabla \cdot \underline{\underline{\tau}}) = 0, \ \forall \underline{\underline{\tau}} \in \mathscr{S}_h. \tag{15}$$

Therefore, given the error estimates (12)-(14), similar results hold for the associated pair of approximation spaces $\{\mathscr{S}_h, \mathscr{U}_h\}$. Precisely,

$$\|\underline{\underline{\sigma}} - \boldsymbol{\Pi}_h \underline{\underline{\sigma}}\|_{L^2(\Omega,\mathbb{M})} \leq Ch^{s+1} \|\underline{\underline{\sigma}}\|_{H^{s+1}(\Omega,\mathbb{M})}, \tag{16}$$

$$\|\underline{\nabla} \cdot \underline{\underline{\sigma}} - \underline{\nabla} \cdot \boldsymbol{\Pi}_h \underline{\underline{\sigma}}\|_{L^2(\Omega,\mathbb{R}^2)} \leq Ch^{l+1} \|\underline{\nabla} \cdot \underline{\underline{\sigma}}\|_{H^{l+1}(\Omega,\mathbb{R}^2)}, \tag{17}$$

$$\|\underline{u} - \Lambda_h \underline{u}\|_{L^2(\Omega,\mathbb{R}^2)} \leq Ch^{t+1} \|\underline{u}\|_{H^{t+1}(\Omega,\mathbb{R}^2)}. \tag{18}$$

Furthermore, let Γ_h denote the L^2-orthogonal projection on $\mathscr{Q}_h$, and m be such that

$$\|q - \Gamma_h q\|_{L^2(\Omega,\mathbb{R})} \leq Ch^{m+1} \|q\|_{H^{m+1}(\Omega,\mathbb{R})}. \tag{19}$$

Note that in the above projection error estimates, the constants appearing on the right hand sides depend only on the shape-regularity factors of the partitions $\mathcal{T}_h$, and on the bounds of $\hat{\boldsymbol{\pi}}^D$ in the reference elements.

4. Error estimates for the mixed weakly symmetric formulation

Given a family of shape-regular meshes $\mathcal{T}_h$ of Ω, let $\mathscr{S}_h \subset H(\mathrm{div},\Omega,\mathbb{M})$, $\mathscr{U}_h \subset L^2(\Omega,\mathbb{R}^2)$ and $\mathscr{Q}_h \subset L^2(\Omega,\mathbb{R})$ be approximation spaces based on $\mathcal{T}_h$ satisfying the Brezzi's conditions for the mixed weakly symmetric formulation, constructed as described in Theorem 1. If $\underline{\underline{\sigma}}_h \in \mathscr{S}_h$, $\underline{u}_h \in \mathscr{U}_h$ and $q_h \in \mathscr{Q}_h$ are approximations of the mixed weakly symmetric formulation (6), then

classic error analyses for stable mixed methods give the following estimate

$$\|\underline{\underline{\sigma}} - \underline{\underline{\sigma}}_h\|_{H(\mathrm{div},\Omega,\mathbb{M})} + \|\underline{u} - \underline{u}_h\|_{L^2(\Omega,\mathbb{R}^2)} + \|q - q_h\|_{L^2(\Omega,\mathbb{R})}$$
$$\leq C \left[\inf_{\underline{\underline{\tau}} \in \mathscr{S}_h} \|\underline{\underline{\sigma}} - \underline{\underline{\tau}}\|_{H(\mathrm{div},\Omega,\mathbb{M})} + \inf_{\underline{\eta} \in \mathscr{U}_h} \|\underline{u} - \underline{\eta}\|_{L^2(\Omega,\mathbb{R}^2)} + \inf_{\varphi \in \mathscr{Q}_h} \|q - \varphi\|_{L^2(\Omega,\mathbb{R})} \right]. \quad (20)$$

However, as shall be revealed by the examples in Section 6, enriched space configurations usually use approximation spaces which may have different orders of accuracy for the different variables. For such cases, the error estimate (20) is not optimal, since it is limited by the less accurate of the approximation spaces. Another analysis can be derived in order to specify error estimates for $\underline{\nabla} \cdot \underline{\underline{\sigma}}$ and $\underline{u}$, individually, in terms of projection errors.

Precisely, considering the bounded projection operators $\boldsymbol{\Pi}_h : \mathbf{H}^{s+1}(\Omega,\mathbb{M}) \to \mathscr{S}_h$, verifying (11), $\Lambda_h : L^2(\Omega,\mathbb{R}^2) \to \mathscr{U}_h$, verifying (15), and the L^2-orthogonal projection $\mathscr{Q}_h$ on Γ_h, the proof of the next results is detailed in Appendix B. It is inspired by similar arguments used in the analysis of mixed methods for Poisson problems, shown in [5, Theorem 6.1]. We also refer to [12] for a similar analysis of a mixed, weakly symmetric, scheme for elasticity using enriched Raviart-Thomas approximations based on simplex meshes.

Theorem 3. *If $\underline{\underline{\sigma}}_h \in \mathscr{S}_h$, $\underline{u}_h \in \mathscr{U}_h$ and $q_h \in \mathscr{Q}_h$ are approximations of the mixed weakly symmetric formulation* (6)*, then the following error estimates hold:*

$$\|\underline{\underline{\sigma}} - \underline{\underline{\sigma}}_h\|_{L^2(\Omega,\mathbb{M})} + \|q - q_h\|_{L^2(\Omega,\mathbb{R})} \leq C(\|\underline{\underline{\sigma}} - \boldsymbol{\Pi}_h\underline{\underline{\sigma}}\|_{L^2(\Omega,\mathbb{M})} + \|q - \Gamma_h q\|_{L^2(\Omega,\mathbb{R})}), \quad (21)$$
$$\|\underline{\nabla} \cdot (\underline{\underline{\sigma}} - \underline{\underline{\sigma}}_h)\|_{L^2(\Omega,\mathbb{R}^2)} \leq C\|\underline{\nabla} \cdot (\underline{\underline{\sigma}} - \boldsymbol{\Pi}_h\underline{\underline{\sigma}})\|_{L^2(\Omega,\mathbb{R}^2)}, \quad (22)$$
$$\|\Lambda_h\underline{u} - \underline{u}_h\|^2_{L^2(\Omega,\mathbb{R}^2)} = (\mathbf{A}(\underline{\underline{\sigma}} - \underline{\underline{\sigma}}_h), \underline{\underline{v}} - \boldsymbol{\Pi}_h\underline{\underline{v}}) + (\Gamma_h q - q, \mathrm{asym}(\boldsymbol{\Pi}_h\underline{\underline{v}})), \quad (23)$$

where $\underline{\underline{v}} \in H^1(\Omega,\mathbb{S})$ and $\underline{w} \in H^2(\Omega,\mathbb{R}^2)$ solve the elasticity problem

$$\begin{aligned} \underline{\nabla} \cdot \underline{\underline{v}} &= \Lambda_h\underline{u} - \underline{u}_h \quad && \text{in } \Omega, \\ \underline{\underline{v}} &= \mathbf{A}^{-1}\underline{\underline{\varepsilon}}(\underline{w}) \quad && \text{in } \Omega, \\ \underline{w} &= \underline{0} && \text{on } \partial\Omega. \end{aligned}$$

Since the inf-sup condition is valid with constants independent of the Poisson ratio, the same holds for the above error estimates. This fact is one main advantage of using mixed methods to solve linear elasticity, allowing to work with materials near the incompressible limit, avoiding the *locking* phenomena.

As a consequence of Theorem 3 and of the projection errors (16)-(19), the following convergence rates hold.

Theorem 4. *Consider approximation space configurations $\{\mathscr{S}_h, \mathscr{U}_h, \mathscr{Q}_h\}$ based on shape regular meshes $\mathcal{T}_h$ of a convex region Ω, obtained from the connection between elasticity elements and stable mixed finite elements for Poisson and Stokes problems, as described in Section 3.1. Let $\boldsymbol{\Pi}_h$ and Λ_h be the projections defined in Section 3.2. If $\underline{\underline{\sigma}}_h \in \mathscr{S}_h$, $\underline{u}_h \in \mathscr{U}_h$, and $q_h \in \mathscr{Q}_h$ satisfy*

(6), *and the functions* $\underline{\underline{\sigma}}$, $\underline{u}$ *and* q, *solutions of* (5), *are regular enough, then the following estimates hold:*

$$\|\underline{\underline{\sigma}} - \underline{\underline{\sigma}}_h\|_{\mathbf{L}^2(\Omega,\mathbb{M})} + \|q - q_h\|_{L^2(\Omega,\mathbb{R})} \leq C\big(h^{s+1}\|\underline{\underline{\sigma}}\|_{\mathbf{H}^{s+1}(\Omega,\mathbb{M})} + h^{m+1}\|q\|_{H^{m+1}(\Omega,\mathbb{R})}\big), \tag{24}$$

$$\|\underline{\nabla} \cdot (\underline{\underline{\sigma}} - \underline{\underline{\sigma}}_h)\|_{L^2(\Omega,\mathbb{R}^2)} \leq\ Ch^{l+1}\|\underline{\nabla} \cdot \underline{\underline{\sigma}}\|_{H^{l+1}(\Omega,\mathbb{R}^2)}, \tag{25}$$

$$\begin{aligned}\|\underline{u} - \underline{u}_h\|_{L^2(\Omega,\mathbb{R}^2)} \leq & C\big(h^{s+2}\|\underline{\underline{\sigma}}\|_{\mathbf{H}^{s+1}(\Omega,\mathbb{M})} + h^{t+1}\|\underline{u}\|_{H^{t+1}(\Omega,\mathbb{R}^2)} \\ & + h^{m+2}\|q\|_{H^{m+1}(\Omega,\mathbb{R})}\big),\end{aligned} \tag{26}$$

where the values of the parameters s, l, t *and* m *are such that* $\mathbb{P}_s(K,\mathbb{M}) \subset S(K,\mathbb{M})$, $\mathbb{P}_l(K,\mathbb{R}^2) \subset \nabla \cdot S(K,\mathbb{M})$, $\mathbb{P}_t(K,\mathbb{R}^2) \subset U(K,\mathbb{R}^2)$, *and* $\mathbb{P}_m(K,\mathbb{R}) \subset Q(K,\mathbb{R})$, $\forall K \in \mathcal{T}_h$.

Proof. Estimates (24) and (25) follow directly by inserting the projection errors (16), (17), and (19) in (21) and (22). Using Cauchy-Schwartz inequality in (23), we obtain

$$\begin{aligned}\|\Lambda_h\underline{u} - \underline{u}_h\|^2_{L^2(\Omega,\mathbb{R}^2)} \leq\ & \|\mathbf{A}(\underline{\underline{\sigma}} - \underline{\underline{\sigma}}_h)\|_{L^2(\Omega,\mathbb{M})}\|\underline{\underline{v}} - \mathbf{\Pi}_h\underline{\underline{v}}\|_{L^2(\Omega,\mathbb{M})} \\ & + \|\Gamma_h q - q\|_{L^2(\Omega,\mathbb{R})}\|\operatorname{asym}(\underline{\underline{v}} - \mathbf{\Pi}_h\underline{\underline{v}})\|_{L^2(\Omega,\mathbb{R})}.\end{aligned}$$

Observing that $\|\underline{\underline{v}}\|_{H^1(\Omega,\mathbb{S})} \approx \|\underline{w}\|_{H^2(\Omega,\mathbb{R}^2)}$ is bounded by $\|\Lambda_h\underline{u} - \underline{u}_h\|_{L^2(\Omega,\mathbb{R}^2)}$, due to the elliptic regularity property, valid for convex Ω, and recalling that $\|\underline{\underline{v}} - \mathbf{\Pi}_h\underline{\underline{v}}\|_{L^2(\Omega,\mathbb{M})} \leq Ch\|\underline{\underline{v}}\|_{H^1(\Omega,\mathbb{M})}$, and $\|\operatorname{asym}(\underline{\underline{v}} - \mathbf{\Pi}_h\underline{\underline{v}})\|_{L^2(\Omega,\mathbb{R})} \leq Ch\|\underline{\underline{v}}\|_{H^1(\Omega,\mathbb{M})}$, we obtain

$$\|\Lambda_h\underline{u} - \underline{u}_h\|_{L^2(\Omega,\mathbb{R}^2)} \leq Ch\left(\|\underline{\underline{\sigma}} - \underline{\underline{\sigma}}_h\|_{L^2(\Omega,\mathbb{M})} + \|\Gamma_h q - q\|_{L^2(\Omega,\mathbb{R})}\right).$$

Finally, the displacement error estimate (26) follows by inserting the above estimate in the triangular inequality

$$\|\underline{u} - \underline{u}_h\|_{L^2(\Omega,\mathbb{R}^2)} \leq \|\underline{u} - \Lambda_h\underline{u}\|_{L^2(\Omega,\mathbb{R}^2)} + \|\Lambda_h\underline{u} - \underline{u}_h\|_{L^2(\Omega,\mathbb{R}^2)},$$

and by recalling the projection errors (18) and (19), and the stress error estimate (24). □

Remark. As a consequence of the observations concerning the leading constants in the projection error estimates (16)-(19), and in the estimates of Theorem 3, the same properties are valid for the leading constants on the right hand sides of the error estimates of Theorem 4. Namely, they only depend on the shape-regularity factors of the partitions $\mathcal{T}_h$, and on the bounds of projections $\hat{\boldsymbol{\pi}}^D$ in the reference elements, being independent of the Poisson ratio.

5. Enriched mixed formulations for Poisson and Stokes problems

This section describes a methodology for restoring the stability of space configurations for Poisson and Stokes problems by the enrichment of the pressure spaces. The original methods are identified by acronyms of the corresponding authors, with an index k referring to the polynomial degree of traces of the corresponding vector functions on the element edges (except

the Poisson-compatible spaces $\mathcal{BDFM}_{k+1}$ for triangles, which follows the original notation [10]). The corresponding enriched versions are indicated by the superscripts $^+$ and $^{++}$.

5.1. Enriched Poisson-compatible space configurations

Consider, in the reference element $\hat{K}$, a Poisson-compatible space configuration with polynomial vector and scalar spaces $\widehat{\mathscr{PC}}_k = \{\hat{\mathbf{V}}_k, \hat{P}_k\}$. The index k refers to the polynomial degree of the normal flux of functions in $\hat{\mathbf{V}}_k$ on the edges in $\partial\hat{K}$. The space $\hat{\mathbf{V}}_k$ can be written as $\hat{\mathbf{V}}_k = \hat{\mathbf{V}}_k^{\partial} \oplus \mathring{\hat{\mathbf{V}}}_k$, where $\hat{\mathbf{V}}_k^{\partial}$ is the set of edge flux functions (those with non-vanishing normal components over $\partial\hat{K}$), and $\mathring{\hat{\mathbf{V}}}_k$ is the set of internal vector functions. As expressed in (3), it is required that the associated scalar space $\hat{P}_k \subset L^2(\hat{K}, \mathbb{R})$ verifies the compatibility condition $\hat{P}_k = \nabla \cdot \hat{\mathbf{V}}_k$.

The enrichment $\widehat{\mathscr{PC}}_k^{n+} = \{\hat{\mathbf{V}}_k^{n+}, \hat{P}_k^{n+}\}$, defined in [14, 18], is constructed as

$$\begin{aligned}\hat{\mathbf{V}}_k^{n+} &= \hat{\mathbf{V}}_k^{\partial} \oplus \mathring{\hat{\mathbf{V}}}_{k+n},\\ \hat{P}_k^{n+} &= \nabla \cdot \hat{\mathbf{V}}_k^{n+} = \hat{P}_{k+n}.\end{aligned}$$

The projection $\boldsymbol{\pi}^{n+}$ for $\hat{\mathbf{V}}_k^{n+}$ can be naturally constructed from the $\boldsymbol{\pi}$ projection of the original spaces, preserving the corresponding property (3) and guaranteeing the stability of the enriched method.

For the current study, the following Poisson-compatible spaces are considered:

Triangular elements

- $\mathcal{BDM}_k$ spaces, with local spaces $V_{\mathcal{BDM}_k}(K, \mathbb{R}^2) = \mathbb{P}_k(K, \mathbb{R}^2)$ and $P_{\mathcal{BDM}_k}(K, \mathbb{R}) = \mathbb{P}_{k-1}(K, \mathbb{R})$.
- Enriched versions: $\mathcal{BDM}_k^+$ $(= \mathcal{BDFM}_{k+1})$, and $\mathcal{BDM}_k^{++}$.

Quadrilateral elements

- $\mathcal{RT}_{[k]}$ spaces, with local spaces $V_{\mathcal{RT}_{[k]}}(K, \mathbb{R}^2) = \mathbb{F}_K^{\mathrm{div}} \hat{\mathbf{V}}_{\mathcal{RT}_{[k]}}$ and $P_{\mathcal{RT}_{[k]}}(K, \mathbb{R}) = \mathbb{F}_K \hat{P}_{\mathcal{RT}_{[k]}}$, where $\hat{\mathbf{V}}_{\mathcal{RT}_{[k]}} = \mathbb{P}_{k+1,k}(\hat{K}, \mathbb{R}) \times \mathbb{P}_{k,k+1}(\hat{K}, \mathbb{R})$ and $\hat{P}_{\mathcal{RT}_{[k]}} = \mathbb{Q}_{k,k}(\hat{K}, \mathbb{R})$.
- Enriched version: $\mathcal{RT}_{[k]}^+$.

The dimension of the local vector spaces is shown in Table 2.

Geometry	Method	$V_k^{\partial}(K, \mathbb{R}^2)$	$\mathring{V}_k(K, \mathbb{R}^2)$	$V(K, \mathbb{R}^2)$
Triangular	$\mathcal{BDM}_k$	$3(k+1)$	$k^2 - 1$	$(k+1)(k+2)$
	$\mathcal{BDM}_k^+$	$3(k+1)$	$(k+1)^2 - 1$	$3 + k(k+5)$
	$\mathcal{BDM}_k^{++}$	$3(k+1)$	$(k+2)^2 - 1$	$(k+1)(k+6)$
Quadrilateral	$\mathcal{RT}_{[k]}$	$4(k+1)$	$2k(k+1)$	$2(k+1)(k+2)$
	$\mathcal{RT}_{[k]}^+$	$4(k+1)$	$2(k+1)(k+2)$	$2(k+1)(k+4)$

Table 2: Dimensions of the local vector spaces $V(K, \mathbb{R}^2) = V^{\partial}(K, \mathbb{R}^2) \oplus \mathring{V}(K, \mathbb{R}^2)$ used in the construction of the stress spaces $S(K, \mathbb{M})$ listed in Table 1.

5.2. Enriched Stokes-compatible space configurations

Consider a Stokes-compatible space configuration $\mathscr{SC}_k = \{\mathscr{W}_k, \mathscr{Q}_k\}$, with local spaces $W_k(K,\mathbb{R}^2)$ and $Q_k(K,\mathbb{R})$. Similarly to the Poisson-compatible case, an enriched version $W_k^+(K,\mathbb{R}^2)$, $Q_k^+(K,\mathbb{R})$ may be constructed by setting $Q_k^+(K,\mathbb{R}) = Q_{k+1}(K,\mathbb{R})$, and by enriching the velocity space with bubble functions $\mathring{B}_{k+1}(K,\mathbb{R}^2)$. Precisely

$$W_k^+(K,\mathbb{R}^2) = W_k(K,\mathbb{R}^2) + \mathring{B}_{k+1}(K,\mathbb{R}^2).$$

The question is how to choose the extra stabilization bubble functions. For triangular meshes, the answer is given in [11, Theorem 2], by taking

$$\mathring{B}_{k+1}(K,\mathbb{R}^2) = b_K \nabla Q_k^+(K,\mathbb{R}),$$

where $b_K = \lambda_1\lambda_2\lambda_3$ is the bubble function defined by the barycentric coordinates λ_i of the triangle K. In order to guarantee stabilization, it is sufficient assume that the original space $\mathscr{W}_k$ contains at least the continuous, piecewise quadratic, functions vanishing on $\partial\Omega$. Similar methodology applies to quadrilateral geometry.

The following Stokes-compatible spaces, and enriched versions of them, shall be considered in the stability analysis for the examples of the next section.

Triangular elements

- Crouzeix-Raviart space ($\mathcal{CR}_k$) for $k = 2, 3$ [13], extended to higher orders in [24]:

$$\mathscr{W}_{\mathcal{CR}_k} = \left\{\underline{w} \in H^1(\Omega,\mathbb{R}^2); \underline{w}|_K \in W_{\mathcal{CR}_k}(K,\mathbb{R}^2),\ K \in \mathcal{T}\right\},$$
$$\mathscr{Q}_{\mathcal{CR}_k} = \left\{q \in L^2(\Omega,\mathbb{R});\ q|_K \in \mathbb{P}_{k-1}(K,\mathbb{R}),\ K \in \mathcal{T}\right\},$$

  with local spaces $W_{\mathcal{CR}_k}(K,\mathbb{R}^2) = \mathbb{P}_k(K,\mathbb{R}^2) + b_K\mathbb{P}_{k-2}(K,\mathbb{R}^2)$. Note that, since $\nabla\mathbb{P}_{k-1}(K,\mathbb{R}) = \mathbb{P}_{k-2}(K,\mathbb{R}^2)$, this space configuration can be viewed as the result of a stabilization by bubble functions.

- Enriched version ($\mathcal{CR}_k^+$), for $k \geq 2$. We propose the following pair of spaces

$$\mathscr{W}_{\mathcal{CR}_k^+} = \left\{\underline{w} \in H^1(\Omega,\mathbb{R}^2); \underline{w}|_K \in W_{\mathcal{CR}_k^+}(K,\mathbb{R}^2),\ K \in \mathcal{T}\right\},$$
$$\mathscr{Q}_{\mathcal{CR}_k^+} = \left\{q \in L^2(\Omega,\mathbb{R});\ q|_K \in \mathbb{P}_k(K,\mathbb{R}),\ K \in \mathcal{T}\right\},$$

  with local spaces

$$W_{\mathcal{CR}_k^+}(K,\mathbb{R}^2) = W_{\mathcal{CR}_k}(K,\mathbb{R}^2) + b_K\nabla\mathbb{P}_k(K,\mathbb{R}).$$

Based on the analysis in [11], the stability of $\mathcal{CR}_k^+$, $k \geq 2$, holds. As far as we understand, this kind of enriched space configuration for Stokes problems is new in the literature.

Quadrilateral elements

- Girault-Raviart space ($\mathcal{GR}_{[k]}$), for $k \geq 2$ [20]:

$$\mathscr{W}_{\mathcal{GR}_{[k]}} = \left\{ \underline{w} \in H^1(\Omega, \mathbb{R}^2); \underline{w}|_K \in W_{\mathcal{GR}_{[k]}}(K, \mathbb{R}^2),\ K \in \mathcal{T} \right\},$$
$$\mathscr{Q}_{\mathcal{GR}_{[k]}} = \left\{ q \in L^2(\Omega, \mathbb{R});\ q|_K \in \mathbb{P}_{k-1}(K, \mathbb{R}),\ K \in \mathcal{T} \right\},$$

  where $W_{\mathcal{GR}_{[k]}}(K, \mathbb{R}^2) = \mathbb{F}_K(\mathbb{Q}_{k,k}(\hat{K}, \mathbb{R}^2))$. According to [20, Theorem 3.2], for regular partitions $\mathcal{T}$, $\{\mathscr{W}_{\mathcal{GR}_{[k]}}, \mathscr{Q}_{\mathcal{GR}_{[k]}}\}$ is stable.

- Enriched version ($\mathcal{GR}^+_{[k]}$), for $k \geq 2$. We propose the following enriched space configuration:

$$\mathscr{W}_{\mathcal{GR}^+_{[k]}} = \left\{ \underline{w} \in H^1(\Omega, \mathbb{R}^2); \underline{w}|_K \in W_{\mathcal{GR}^+_{[k]}}(K, \mathbb{R}^2),\ K \in \mathcal{T} \right\},$$
$$\mathscr{Q}_{\mathcal{GR}^+_{[k]}} = \left\{ q \in L^2(\Omega, \mathbb{R});\ q|_K \in \mathbb{P}_k(K, \mathbb{R}),\ K \in \mathcal{T} \right\}.$$

  The local spaces

$$W_{\mathcal{GR}^+_{[k]}}(K, \mathbb{R}^2) = W_{\mathcal{GR}_{[k]}}(K, \mathbb{R}^2) + \mathring{B}_{k+1}(K, \mathbb{R}^2),$$

  are obtained by adding the bubble functions $\mathring{B}_{k+1}(K, \mathbb{R}^2) = \mathbb{F}_K\left(\mathring{\hat{B}}_{k+1}(\hat{K}, \mathbb{R}^2)\right)$, with

$$\mathring{B}_{k+1}(\hat{K}, \mathbb{R}^2) = \{b_{\hat{K}}\underline{\hat{w}};\ \underline{\hat{w}} \in \mathbb{Q}_{k-1,k-1}(\hat{K}, \mathbb{R}^2)\} \subset \mathbb{Q}_{k+1,k+1}(\hat{K}, \mathbb{R}^2),$$

  $b_{\hat{K}}$ being the basic bubble function on $\hat{K}$, i.e., $b_{\hat{K}}(\hat{x}, \hat{y}), = U(\hat{x})U(\hat{y}) \in \mathbb{Q}_{2,2}(\hat{K}, \mathbb{R})$, $U \in \mathbb{P}_2([0,1], \mathbb{R})$, $U(0) = U(1) = 0$. Then, on each element $K \in \mathcal{T}$, one has

$$\begin{aligned}\mathring{B}_{k+1}(K, \mathbb{R}^2) &= \{\mathbb{F}_K(b_{\hat{K}})\mathbb{F}_K(\underline{\hat{w}});\ \underline{\hat{w}} \in \mathbb{Q}_{k-1,k-1}(\hat{K}, \mathbb{R}^2)\} \\ &= \{b_K\mathbb{F}_K(\underline{\hat{w}});\ \underline{\hat{w}} \in \mathbb{Q}_{k-1,k-1}(\hat{K}, \mathbb{R}^2)\}.\end{aligned}$$

  It is known that $\mathbb{F}_K(\mathbb{Q}_{k-1,k-1}(\hat{K}, \mathbb{R}^2))$ contains $\mathbb{P}_{k-1}(K, \mathbb{R}^2) = \nabla\mathbb{P}_k(K, \mathbb{R})$ (see [4, Theorem 3]). Consequently, according to the Corollary of Theorem 2 in [11], the stability of the enriched Stokes space configuration $\{\mathscr{W}_{\mathcal{GR}^+_{[k]}}, \mathscr{Q}_{\mathcal{GR}^+_{[k]}}\}$ holds. As far as we understand, the enriched space configuration $\mathcal{GR}^+_{[k]}$ is new in the literature concerning the Stokes problem.

6. Enriched stable approximations for linear elasticity with weak stress symmetry

In this section the five examples of stable space configurations for the mixed formulation of linear elasticity with weak stress symmetry indicated in Table 1 are discussed. Numerical tests using these spaces are shown in the following section. Different families of stable spaces for the mixed formulation of the Poisson problem are used in the construction of the space configuration for mixed elasticity: three for triangles and two for quadrilateral elements. Precisely, the Poisson-compatible approximation spaces are of type $\mathcal{BDM}_k$, $\mathcal{BDM}^+_k$ and $\mathcal{BDM}^{++}_k$ for

triangular elements, and of type $\mathcal{RT}_{[k]}$ and $\mathcal{RT}^{+}_{[k]}$, as described in Section 5, for quadrilateral elements. The resulting elasticity families of spaces are identified by the name of the corresponding Poisson-compatible space used in their definition. Two examples of Stokes-compatible spaces, one for each geometry, and new enriched versions of them, as introduced in Section 5.2, shall be used to justify the stability of the analyzed examples for elasticity problems, following the guidelines of Theorem 1.

The accuracy orders of the new schemes shall be derived, based on the error analysis of the previous sections, determined by the parameters s, l, t and m, defining the convergence rates for the projections (12)-(14) and (19). For all cases, the region Ω is supposed to be convex, and the meshes are assumed to be shape regular.

Finally, after applying the error estimates of Theorem 4 to the considered configurations, we summarize the resulting rates of convergence for the variables $\underline{\underline{\sigma}}, \underline{u}, \underline{\nabla} \cdot \underline{\underline{\sigma}}$, and q in Table 3, both for affine elements and for non-affine quadrilateral elements mapped by bilinear transformations.

Geometry	P-method	$\underline{\underline{\sigma}}$		$\underline{u}$		$\underline{\nabla} \cdot \underline{\underline{\sigma}}$		q	
Triangular	$\mathcal{BDM}_k$	k		k		k		k	
	$\mathcal{BDM}_k^+$	$k+1$		$k+1$		$k+1$		$k+1$	
	$\mathcal{BDM}_k^{++}$	$k+1$		$k+2$		$k+2$		$k+1$	
Quadrilateral		A	N-A	A	NA	A	NA	A	NA
	$\mathcal{RT}_{[k]}$	$k+1$	$k+1$	$k+1$	$k+1$	$k+1$	k	$k+1$	$k+1$
	$\mathcal{RT}^{+}_{[k]}$	$k+1$	$k+1$	$k+2$	$k+2$	$k+2$	$k+1$	$k+1$	$k+1$

Table 3: Orders of convergence in L^2-norms that can be achieved by the combination of stable finite element spaces $\mathscr{S} \subset H(\mathrm{div}, \Omega, \mathbb{M}), \mathscr{U} \subset L^2(\Omega, \mathbb{R}^2)$, $\mathscr{Q} \subset L^2(\Omega, \mathbb{R})$ indicated in Table 1, when applied to the mixed method for linear elasticity with weakly imposed stress symmetry. The spaces are constructed from Poisson-compatible methods (P-method) based on triangular, affine (A) and non-affine (N-A) quadrilateral meshes (these mapped by bilinear transformations).

6.1. Triangular elements

Three families of stable approximations for linear elasticity with weak stress symmetry are presented for triangular meshes. These families are based on the Poisson-compatible $\mathcal{BDM}_k$ spaces, or on some enriched versions of them.

6.1.1. Based on $\mathcal{BDM}_k$ spaces, $k \geq 1$

One classic space configuration is the Arnold-Falk-Winther family [6], defined as

$$\mathscr{E}_{\mathcal{BDM}_k} = \{\mathscr{S}_{\mathcal{BDM}_k}, \mathscr{U}_{\mathcal{BDM}_k}, \mathscr{Q}_{\mathcal{BDM}_k}\},$$

with

$$\begin{aligned}
\mathscr{S}_{\mathcal{BDM}_k} &= \left\{ \underline{\underline{\tau}} \in H(\mathrm{div}, \Omega, \mathbb{M});\ \underline{\underline{\tau}}|_K \in \mathbb{P}_k(K, \mathbb{M}),\ K \in \mathcal{T} \right\}, \\
\mathscr{U}_{\mathcal{BDM}_k} &= \left\{ \underline{u} \in L^2(\Omega, \mathbb{R}^2);\ \underline{u}|_K \in \mathbb{P}_{k-1}(K, \mathbb{R}^2),\ K \in \mathcal{T} \right\}, \\
\mathscr{Q}_{\mathcal{BDM}_k} &= \left\{ q \in L^2(\Omega, \mathbb{R});\ q|_K \in \mathbb{P}_{k-1}(K, \mathbb{R}),\ K \in \mathcal{T} \right\}.
\end{aligned}$$

For this case, $s = k$, $l = t = m = k - 1$.

6.1.2. Based on $\mathcal{BDM}_k^+$ spaces, $k \geq 1$

Consider the enriched space configuration $\mathcal{BDM}_k^+$ for the mixed Poisson problem (corresponding to the classic $\mathcal{BDFM}_{k+1}$ family). By construction, the local flux space $V_{\mathcal{BDM}_k^+}(K, \mathbb{R}^2)$ contains $V_{\mathcal{BDM}_k}(K, \mathbb{R}^2)$, and is obtained by including all internal (bubble) functions of polynomial degree $k+1$. This fact guarantees stability for pressure local spaces in $\mathbb{P}_k$ (instead of $\mathbb{P}_{k-1}$, as in the case for the original $\mathcal{BDM}_k$ case).

For the mixed formulation of linear elasticity with weak stress symmetry, we propose the approximation spaces

$$\begin{aligned}
\mathscr{S}_{\mathcal{BDM}_k^+} &= \left\{ \underline{\underline{\tau}} \in H(\mathrm{div}, \Omega, \mathbb{M});\ \underline{\underline{\tau}}|_K \in S_{\mathcal{BDM}_k^+}(K, \mathbb{M}),\ K \in \mathcal{T} \right\}, \\
\mathscr{U}_{\mathcal{BDM}_k^+} &= \left\{ \underline{u} \in L^2(\Omega, \mathbb{R}^2);\ \underline{u}|_K \in \mathbb{P}_k(K, \mathbb{R}^2),\ K \in \mathcal{T} \right\}, \\
\mathscr{Q}_{\mathcal{BDM}_k^+} &= \left\{ q \in L^2(\Omega, \mathbb{R});\ q|_K \in \mathbb{P}_k(K, \mathbb{R}),\ K \in \mathcal{T} \right\}.
\end{aligned}$$

Note that for $k = 1$ this space configuration corresponds to the Example 3.4 in [17].

Recall that the enhanced internal local space $\mathring{V}_{\mathcal{BDM}_k^+}(K, \mathbb{R}^2)$ includes the bubble functions necessary to stabilize the Poisson formulation with local pressure spaces in $\mathbb{P}_k(K, \mathbb{R})$, but it also has all divergence-free bubble functions of $\mathbb{P}_{k+1}(K, \mathbb{R}^2)$, denoted by $\delta V_{k+1}(K, \mathbb{R}^2)$. According to [10, Lemma 3.2], $\delta V_{k+1}(K, \mathbb{R}^2)$ is characterized by

$$\delta V_{k+1}(K, \mathbb{R}^2) = \left\{ \underline{\nabla} \times (b_K w),\ w \in \mathbb{P}_{k-1}(K, \mathbb{R}) \right\}.$$

Therefore, in order to guarantee that

$$\mathscr{E}_{\mathcal{BDM}_k^+} = \{ \mathscr{S}_{\mathcal{BDM}_k^+}, \mathscr{U}_{\mathcal{BDM}_k^+}, \mathscr{Q}_{\mathcal{BDM}_k^+} \}$$

is a stable configuration for approximation of the mixed elasticity problem, by the application of Theorem 1 it is enough to show that a Stokes-compatible configuration $\{\mathscr{W}, \mathscr{Q}\}$ exists with local pressure space $Q(K, \mathbb{R}) = \mathbb{P}_k(K, \mathbb{R})$ and a velocity local space $W(K, \mathbb{R}^2)$ verifying $\underline{\underline{\nabla}} \times W(K, \mathbb{R}^2) \subset S_{\mathcal{BDM}_k^+}(K, \mathbb{M})$. A space configuration that satisfies this properties is the Crouzeix-Raviart space $\mathcal{CR}_{k+1} = \{\mathscr{W}_{\mathcal{CR}_{k+1}},\ \mathscr{Q}_{\mathcal{CR}_{k+1}}\}$. Consequently, by the application of Theorem 1, the space configuration $\mathscr{E}_{\mathcal{BDM}_k^+}$ results to be stable for the elasticity problem (noting that $\mathscr{Q}_{\mathcal{BDM}_k^+} = \mathscr{Q}_{\mathcal{CR}_{k+1}}$). Concerning the convergence parameters for $\mathscr{E}_{\mathcal{BDM}_k^+}$, it is clear that $s = l = t = m = k$.

6.1.3. Based on $\mathcal{BDM}_k^{++}$ spaces, $k \geq 1$

Consider the enriched $\mathcal{BDM}_k^{++} = \mathcal{BDM}_k^{2+}$ space configuration for the mixed Poisson problem, as described in [18] and define

$$\begin{aligned}
\mathscr{S}_{\mathcal{BDM}_k^{++}} &= \left\{ \underline{\underline{\tau}} \in H(\mathrm{div}, \Omega, \mathbb{M});\ \underline{\underline{\tau}}|_K \in S_{\mathcal{BDM}_k^{++}}(K, \mathbb{M}),\ K \in \mathcal{T} \right\}, \\
\mathscr{U}_{\mathcal{BDM}_k^{++}} &= \left\{ \underline{u} \in L^2(\Omega, \mathbb{R}^2);\ \underline{u}|_K \in \mathbb{P}_{k+1}(K, \mathbb{R}^2),\ K \in \mathcal{T} \right\}.
\end{aligned}$$

By construction, the local space $S_{\mathcal{BDM}_k^{++}}(K,\mathbb{M})$ contains $S_{\mathcal{BDM}_k^{+}}(K,\mathbb{M})$, implying that $\underline{\underline{\nabla}} \times \mathscr{W}_{\mathcal{CR}_{k+1}} \subset \mathscr{S}_{\mathcal{BDM}_k^{++}}$ also holds. Therefore, the stability for the space configuration

$$\mathscr{E}_{\mathcal{BDM}^{\sim}_{[k]}} = \{\mathscr{S}_{\mathcal{BDM}_k^{++}}, \mathscr{U}_{\mathcal{BDM}_k^{++}}, \mathscr{Q}_{\mathcal{BDM}_k^{+}}\}$$

holds as a consequence of Theorem 1.

However, recall that the enhanced local vector space $V_{\mathcal{BDM}_k^{++}}(K,\mathbb{R}^2)$ includes all bubble functions in $\mathbb{P}_{k+2}(K,\mathbb{R}^2)$, i.e., those necessary to stabilize the Poisson formulation with local pressures in $\mathbb{P}_{k+1}(K,\mathbb{R})$ and also divergence-free bubble functions, which, according to [10, Lemma 3.2], are identified as the elements of the set

$$\delta V_{k+2}(K,\mathbb{R}^2) = \left\{\underline{\nabla} \times (b_K w),\ w \in \mathbb{P}_k(K,\mathbb{R})\right\}.$$

Therefore, there is room to improve the choice of the approximation space for the rotation. By setting

$$\mathscr{Q}_{\mathcal{BDM}_k^{++}} = \left\{q \in L^2(\Omega,\mathbb{R});\ q|_K \in \mathbb{P}_{k+1}(K,\mathbb{R}),\ K \in \mathcal{T}\right\} = \mathscr{Q}_{\mathcal{CR}_{k+1}^{+}}$$

and following the stability analysis done for the space configuration based on $\mathcal{BDM}_k^{+}$, we conclude that an appropriate choice for the Stokes-compatible spaces $\{\mathscr{W},\mathscr{Q}\}$ to be used for the construction of the $\mathcal{BDM}_k^{++}$ configuration needs to provide a local pressure space $Q(K,\mathbb{R}) = \mathbb{P}_{k+1}(K,\mathbb{R})$ and a local velocity space $W(K,\mathbb{R}^2)$ such that

$$\underline{\underline{\nabla}} \times W(K,\mathbb{R}^2) \subset S_{\mathcal{BDM}_k^{++}}(K,\mathbb{M}).$$

The enriched Stokes-compatible pair $\{\mathscr{W}_{\mathcal{CR}_{k+1}^{+}}, \mathscr{Q}_{\mathcal{CR}_{k+1}^{+}}\}$ verifies these properties and, therefore, the space configuration

$$\mathscr{E}_{\mathcal{BDM}_k^{++}} = \{\mathscr{S}_{\mathcal{BDM}_k^{++}}, \mathscr{U}_{\mathcal{BDM}_k^{++}}, \mathscr{Q}_{\mathcal{BDM}_k^{++}}\}$$

results to be stable, according to Theorem 1.

For this case, the accuracy of the approximations is determined by the parameters $s = k$, $l = t = m = k+1$.

6.2. Quadrilateral meshes

In this section, two families of stable approximations for linear elasticity with weak stress symmetry are considered for quadrilateral meshes, one based on the Poisson-compatible $\mathcal{RT}_{[k]}$ spaces, and a new one based on their enriched version, $\mathcal{RT}^{+}_{[k]}$.

6.2.1. Based on the $\mathcal{RT}_{[k]}$ spaces, $k \geq 1$

As proposed in [1], let the space configuration

$$\mathscr{S}_{\mathcal{RT}_{[k]}} = \left\{ \underline{\underline{\tau}} \in H(\mathrm{div}, \Omega, \mathbb{M});\ \underline{\underline{\tau}}|_K \in S_{\mathcal{RT}_{[k]}}(K, \mathbb{M}),\ K \in \mathcal{T} \right\},$$
$$\mathscr{U}_{\mathcal{RT}_{[k]}} = \left\{ \underline{u} \in L^2(\Omega, \mathbb{R}^2);\ \underline{u}|_K \in U_{\mathcal{RT}_{[k]}}(K, \mathbb{R}^2),\ K \in \mathcal{T} \right\},$$
$$\mathscr{Q}_{\mathcal{RT}_{[k]}} = \left\{ q \in L^2(\Omega, \mathbb{R});\ q|_K \in \mathbb{P}_k(K, \mathbb{R}),\ K \in \mathcal{T} \right\}.$$

Taking the Stokes-stable family $\mathcal{GR}_{[k+1]}$, with $\hat{W}_{\mathcal{GR}_{[k+1]}} = \mathbb{Q}_{k+1,k+1}(\hat{K}, \mathbb{R}^2)$, the inclusion $\underline{\underline{\nabla}} \times \mathscr{W}_{\mathcal{GR}_{[k+1]}} \subset \mathscr{S}_{\mathcal{RT}_{[k]}}$ is easily verified [1], guaranteeing the hypotheses of Theorem 1, and implying that

$$\mathscr{E}_{\mathcal{RT}_{[k]}} = \{\mathscr{S}_{\mathcal{RT}_{[k]}}, \mathscr{U}_{\mathcal{RT}_{[k]}}, \mathscr{Q}_{\mathcal{RT}_{[k]}}\}$$

is a stable space configuration for the mixed formulation for linear elasticity with weak stress symmetry.

On affine quadrilateral meshes, all variables have the same order of accuracy, determined by equal parameters $s = l = t = m = k$. For quadrilateral meshes with elements mapped by bilinear transformations, the order of accuracy of the divergence approximation decreases one unit [5], i.e., $s = t = m = k$, but $l = k - 1$.

6.2.2. Based on the enriched $\mathcal{RT}^+_{[k]}$ spaces, $k \geq 1$

Consider the enriched $\mathcal{RT}^+_{[k]}$ space configuration for the mixed Poisson problem, as described in [18]. Precisely, $P_{\mathcal{RT}^+_{[k]}}(K, \mathbb{R}) = P_{\mathcal{RT}_{[k+1]}}(K, \mathbb{R})$, and

$$V_{\mathcal{RT}^+_{[k]}}(K, \mathbb{R}^2) = V^{\partial}_{\mathcal{RT}_{[k]}}(K, \mathbb{R}^2) \oplus \mathring{V}_{\mathcal{RT}_{[k+1]}}(K, \mathbb{R}^2).$$

Accordingly, we propose the following enriched space configuration for stress and displacement:

$$\mathscr{S}_{\mathcal{RT}^+_{[k]}} = \{\underline{\underline{\tau}} \in H(\mathrm{div}, \Omega, \mathbb{M});\ \underline{\underline{\tau}}|_K \in S_{\mathcal{RT}^+_{[k]}}(K, \mathbb{M}),\ K \in \mathcal{T}\},$$
$$\mathscr{U}_{\mathcal{RT}^+_{[k]}} = \{\underline{u} \in L^2(\Omega, \mathbb{R}^2);\ \underline{u}|_K \in U_{\mathcal{RT}^+_{[k]}}(K, \mathbb{R}^2),\ K \in \mathcal{T}\}.$$

By construction, the flux approximation space $V_{\mathcal{RT}^+_{[k]}}(K, \mathbb{R}^2)$ contains $V_{\mathcal{RT}_{[k]}}(K, \mathbb{R}^2)$, implying that $\underline{\underline{\nabla}} \times \mathscr{W}_{\mathcal{GR}_{[k+1]}} \subset \mathscr{S}_{\mathcal{RT}^+_{[k]}}$ also holds. Therefore, by Theorem 1, the approximation space configuration

$$\mathscr{E}_{\mathcal{RT}^{\sim}_{[k]}} = \{\mathscr{S}_{\mathcal{RT}^+_{[k]}}, \mathscr{U}_{\mathcal{RT}^+_{[k]}}, \mathscr{Q}_{\mathcal{RT}_{[k]}}\}$$

is stable. The accuracy orders obtained using the $\mathscr{E}_{\mathcal{RT}^{\sim}_{[k]}}$ space configuration are determined by the parameters $s = m = k$ and $t = k + 1$. For the divergence of the stress, $l = k + 1$ in the case of affine meshes, and $l = k$ for general bilinearly mapped quadrilaterals.

In order to guarantee that

$$\mathscr{E}_{\mathcal{RT}^+_{[k]}} = \{\mathscr{S}_{\mathcal{RT}^+_{[k]}}, \mathscr{U}_{\mathcal{RT}^+_{[k]}}, \mathscr{Q}_{\mathcal{RT}_{[k+1]}}\}$$

is a stable configuration as well, take the enriched Stokes-stable family $\mathcal{GR}^+_{[k+1]}$, as described in Section 5.2, with

$$W_{\mathcal{GR}^+_{[k+1]}}(K,\mathbb{R}^2) = W_{\mathcal{GR}_{[k+1]}}(K,\mathbb{R}^2) + \mathring{B}_{k+2}(K,\mathbb{R}^2),$$
$$Q_{\mathcal{GR}^+_{[k+1]}}(K) = \mathbb{P}_{k+1}(K),$$

where the stabilizing bubbles functions $\mathring{B}_{k+2}(K,\mathbb{R}^2) = \mathbb{F}_K\left[\mathring{B}_{k+2}(\hat{K},\mathbb{R}^2)\right]$ are such that $\mathring{B}_{k+2}(\hat{K},\mathbb{R}^2)_3 \subset \mathbb{Q}_{k+2,k+2}(\hat{K},\mathbb{R}^2)$. Therefore,

$$\underline{\underline{\nabla}} \times W_{\mathcal{GR}^+_{[k+1]}}(K,\mathbb{R}^2) = \underline{\underline{\nabla}} \times W_{\mathcal{GR}_{[k+1]}}(K,\mathbb{R}^2) + \underline{\underline{\nabla}} \times \mathring{B}_{k+2}(K,\mathbb{R}^2).$$

From the stability analysis of $\mathscr{E}_{\mathcal{RT}_{[k]}}$ in [1], it is already known that $\underline{\underline{\nabla}} \times W_{\mathcal{GR}_{[k+1]}}(K,\mathbb{R}^2) \subset S_{\mathcal{RT}_{[k]}}(K,\mathbb{M}) \subset S_{\mathcal{RT}^+_{[k]}}(K,\mathbb{M})$. For the stabilizing bubble term, observe that

$$\begin{aligned}\underline{\underline{\nabla}} \times \mathring{B}_{k+2}(K,\mathbb{R}^2) &= \underline{\underline{\nabla}} \times \mathbb{F}_K\left[\mathring{B}_{k+2}(\hat{K},\mathbb{R}^2)\right] \\ &= \mathbb{F}^{\mathrm{div}}_K\left[\underline{\underline{\nabla}} \times \mathring{B}_{k+2}(\hat{K},\mathbb{R}^2)\right] \\ &\subset \mathbb{F}^{\mathrm{div}}_K\left[\underline{\underline{\nabla}} \times \mathbb{Q}_{k+2,k+2}(\hat{K},\mathbb{R}^2)\right].\end{aligned}$$

According to [10, Lemma 3.3], $\mathbb{F}^{\mathrm{div}}_K\left[\underline{\nabla} \times \mathbb{Q}_{k+2,k+2}(\hat{K},\mathbb{R})\right]$ is the space of divergence-free functions in $V_{\mathcal{RT}_{[k+1]}}(K,\mathbb{R}^2)$. Furthermore, since the functions in $\mathring{B}_{k+2}(K,\mathbb{R}^2)$ vanish over ∂K, then we conclude that $\underline{\underline{\nabla}} \times \mathring{B}_{k+2}(K,\mathbb{R}^2) \subset \mathring{S}_{\mathcal{RT}_{[k+1]}}(K,\mathbb{M}) = \mathring{S}_{\mathcal{RT}^+_{[k]}}(K,\mathbb{M})$. Consequently, the inclusion $\underline{\underline{\nabla}} \times W_{\mathcal{GR}^+_{[k+1]}} \subset \mathscr{S}_{\mathcal{RT}^+_{[k]}}$ is verified. Applying Theorem 1, the approximation space configuration $\mathscr{E}_{\mathcal{RT}^+_{[k]}}$ results to be stable, with

$$\mathscr{Q}_{\mathcal{RT}^+_{[k]}} = \left\{q \in L^2(\Omega,\mathbb{R});\ q|_K \in \mathbb{P}_{k+1}(K,\mathbb{R}),\ K \in \mathcal{T}\right\} = \mathscr{Q}_{\mathcal{RT}_{[k+1]}}.$$

The accuracy orders obtained using the $\mathscr{E}_{\mathcal{RT}^+_{[k]}}$ space configuration are determined by the parameters $s = k$ and $t = m = k+1$. For the divergence of the stress, $l = k+1$ in the case of affine meshes, and $l = k$ for general bilinearly mapped quadrilaterals.

Other possible choices for the local space $\mathscr{Q}(K,\mathbb{R})$, for affine quadrilaterals

The comparison with some other Stokes-compatible spaces existing in the literature suggests other possible choices for the space $\mathscr{Q}$, to be used for weakly enforcing the symmetry of the stress.

In [29], the authors introduced a general methodology for the construction of Stokes-compatible methods based on affine quadrilaterals. They also presented six methods; some of them can be used to show that the tensor and displacement approximations for elasticity based on Poisson-compatible spaces $\mathcal{RT}_{[k]}$ and $\mathcal{RT}^+_{[k]}$ for such meshes can be combined with different spaces $\mathscr{Q}$ for the variable q to construct stable configurations for approximation of the elasticity problem.

1. Spaces based on $\mathcal{RT}_{[k]}$, with $Q(\hat{K},\mathbb{R}) = \mathbb{Q}_{k-1,k-1}(\hat{K},\mathbb{R}) \cup \mathbb{P}_k(\hat{K},\mathbb{R})$: Consider the Stokes-compatible configuration $SS_{k+1}(6)$, indicated as Method 6 in [29]. It uses as local spaces $W_{SS_{k+1}(6)}(\hat{K},\mathbb{R}^2) = \mathbb{Q}_{k+1,k+1}(\hat{K},\mathbb{R}^2) = W_{\mathcal{GR}_{[k+1]}}(\hat{K},\mathbb{R}^2)$, and $Q_{SS_{k+1}(6)}(\hat{K},\mathbb{R}) = \mathbb{Q}_{k-1,k-1}(\hat{K},\mathbb{R}) \cup \mathbb{P}_k(\hat{K},\mathbb{R})$, which is the maximal pressure space corresponding to this kind of velocity space. Therefore, the space configuration $\{\mathscr{S}_{\mathcal{RT}_{[k]}},\ \mathscr{U}_{\mathcal{RT}_{[k]}},\ \mathscr{Q}_{SS_{k+1}(6)}\}$ is stable for the elasticity mixed formulation with weak symmetry.

2. Spaces based on $\mathcal{RT}^+_{[k]}$, with $Q(\hat{K},\mathbb{R}) = \mathbb{Q}_{k,k}(\hat{K},\mathbb{R}) \cup \mathbb{P}_{k+1}(\hat{K},\mathbb{R})$: Consider the Stokes-compatible configuration with local spaces $W_{\mathcal{GR}^+_{[k+1]}}(K,\mathbb{R}^2)$ and $Q(\hat{K},\mathbb{R}) = \mathbb{Q}_{k,k}(\hat{K},\mathbb{R}) \cup \mathbb{P}_{k+1}(\hat{K},\mathbb{R})$, for affine quadrilateral meshes. Since $\underline{\underline{\nabla}} \times \mathscr{W}_{\mathcal{GR}^+_{[k+1]}} \subset \mathscr{S}_{\mathcal{RT}^+_{[k]}}$, approximations with local spaces $Q(\hat{K},\mathbb{R}) = \mathbb{Q}_{k,k}(\hat{K},\mathbb{R}) \cup \mathbb{P}_{k+1}(\hat{K},\mathbb{R})$ are also an option for weakly enforcing stress symmetry on the $\mathcal{RT}^+_{[k]}$ context, given that the mesh is based on affine quadrilaterals.

It should be observed that these two options do not increase the convergence order of the approximations. However, the magnitude of the error for q may be reduced when $Q(\hat{K},\mathbb{R}) = \mathbb{Q}_{k-1,k-1}(\hat{K},\mathbb{R}) \cup \mathbb{P}_k(\hat{K},\mathbb{R})$ or $Q(\hat{K},\mathbb{R}) = \mathbb{Q}_{k,k}(\hat{K},\mathbb{R}) \cup \mathbb{P}_{k+1}(\hat{K},\mathbb{R})$ are used in the $\mathcal{RT}_{[k]}$ and $\mathcal{RT}^+_{[k]}$ contexts, respectively.

6.3. Related spaces in the literature

In this section we recall some known related stable space configurations for the mixed formulation of linear elasticity with weak stress symmetry.

6.3.1. Three families for triangles

The principle used in [28] to construct enhanced space configurations for elasticity problems is based on the enrichment of Poisson-compatible spaces with divergence-free functions. This strategy allows for an improvement in the space that is used to weakly impose the symmetry. For instance, the example analyzed there in detail is based on the $\mathcal{BDM}_k$ space for triangles.

Configuration based on $\mathcal{BDM}_k$ spaces:

Consider the space configuration $\mathscr{E}_{S-\mathcal{BDM}_k}$, analyzed in [28]:

$$\mathscr{S}_{S-\mathcal{BDM}_k} = \left\{\underline{\underline{\tau}} \in H(\mathrm{div},\Omega,\mathbb{M});\ \underline{\underline{\tau}}|_K \in \mathbb{P}_k(K,\mathbb{M}) + \delta S_{k+1}(K,\mathbb{M}),\ K \in \mathcal{T}\right\},$$
$$\mathscr{U}_{S-\mathcal{BDM}_k} = \left\{\underline{u} \in L^2(\Omega,\mathbb{R}^2);\ \underline{u}|_K \in \mathbb{P}_{k-1}(K,\mathbb{R}^2),\ K \in \mathcal{T}\right\},$$
$$\mathscr{Q}_{S-\mathcal{BDM}_k} = \left\{q \in L^2(\Omega,\mathbb{R});\ q|_K \in \mathbb{P}_k(K,\mathbb{R}),\ K \in \mathcal{T}\right\},$$

where $\delta S_{k+1}(K,\mathbb{M}) = \{\underline{\underline{\nabla}} \times (b_K \underline{w}),\ \underline{w} \in \mathbb{P}_{k-1}(K,\mathbb{R}^2)\} \subset \mathbb{P}_{k+1}(K,\mathbb{M})$.

A confront of this space configuration with the Arnold-Falk-Winther family $\mathscr{E}_{\mathcal{BDM}_k}$, proposed in [6] and described in Section 6.1.1 shows that the enrichment of the local spaces $\mathbb{P}_k(K,\mathbb{M})$ with the divergence free space $\delta S_{k+1}(K,\mathbb{M})$ allows the $\mathscr{E}_{S-\mathcal{BDM}_k}$ family to stably use richer local approximations in $Q(K,\mathbb{R}) = \mathbb{P}_k(K,\mathbb{R})$ for the rotation variable, instead of $\mathbb{P}_{k-1}(K,\mathbb{R})$, as in the former $\mathscr{E}_{\mathcal{BDM}_k}$ case.

Note also that the rows of the extra term $\delta S_{k+1}(K,\mathbb{M})$ are the divergence free vector functions of $\mathbb{P}_{k+1}(K,\mathbb{R}^2)$, with vanishing normal components over ∂K (see [10, Lemma 3.2]). Therefore, $\mathbb{P}_k(K,\mathbb{M}) \oplus \delta S_{k+1}(K,\mathbb{M}) \subsetneq S_{\mathcal{BDM}_k^+}(K,\mathbb{M})$.

Configuration based on $\mathcal{RT}_k$ spaces

As argued in [28], a similar technique for stabilization by adding divergence-free bubble functions can be applied to other space configurations based on Poisson-compatible spaces. For instance, the space configuration $\mathscr{E}_{S-\mathcal{RT}_k}$ is based on the $\mathcal{RT}_k$ space for simplicial elements:

$$\begin{aligned}
\mathscr{S}_{S-\mathcal{RT}_k} &= \left\{ \underline{\underline{\tau}} \in H(\mathrm{div},\Omega,\mathbb{M});\ \underline{\underline{\tau}}|_K \in S_{\mathcal{RT}_k}(K,\mathbb{M}) + \delta S_{k+1}(K,\mathbb{M}),\ K \in \mathcal{T} \right\},\\
\mathscr{U}_{S-\mathcal{RT}_k} &= \left\{ \underline{u} \in L^2(\Omega,\mathbb{R}^2);\ \underline{u}|_K \in \mathbb{P}_k(K,\mathbb{R}^2),\ K \in \mathcal{T} \right\},\\
\mathscr{Q}_{S-\mathcal{RT}_k} &= \left\{ q \in L^2(\Omega,\mathbb{R});\ q|_K \in \mathbb{P}_k(K,\mathbb{R}),\ K \in \mathcal{T} \right\}.
\end{aligned}$$

A confront of this space configuration with $\mathscr{E}_{S-\mathcal{BDM}_k}$ leads to the observation that the use of enriched local spaces $S_{\mathcal{RT}_k}(K,\mathbb{M})$, instead of $\mathbb{P}_k(K,\mathbb{M})$, allows the $\mathscr{E}_{S-\mathcal{RT}_k}$ family to use the richer local spaces $\mathbb{P}_k(K,\mathbb{R}^2)$ for approximation of the displacement variable, instead of $\mathbb{P}_{k-1}(K,\mathbb{R}^2)$ as in the former $\mathscr{E}_{S-\mathcal{BDM}_k}$ case.

It can also be observed that the local vector spaces $V_{\mathcal{RT}_k}(K,\mathbb{R}^2)$ (with dimension $(k+1)(k+3)$) are contained in $V_{\mathcal{BDM}_k^+}(K,\mathbb{R}^2)$ (= $\mathcal{BDFM}_{k+1}$ space, with dimension $k(k+5)+3$). They share the same edge component, and their divergence is the space $\mathbb{P}_k(K,\mathbb{R})$. In fact, they differ by a divergence-free vector space of dimension k included in $\mathbb{P}_{k+1}(K,\mathbb{R}^2)$. Since $\mathring{V}_{\mathcal{BDM}_k^+}(K,\mathbb{R}^2)$ contains all the internal vector functions in $\mathbb{P}_{k+1}(K,\mathbb{R}^2)$, including the ones in $\mathring{V}_{\mathcal{RT}_k}(K,\mathbb{R}^2)$, and the remaining divergence-free ones, we conclude that $S_{\mathcal{RT}_k}(K,\mathbb{M}) + \delta S_{k+1}(K,\mathbb{M}) = S_{\mathcal{BDM}_k^+}(K,\mathbb{M})$. Therefore, the space configurations $\mathscr{E}_{S-\mathcal{RT}_k}$ and $\mathscr{E}_{\mathcal{BDM}_k^+}$ for elasticity with weakly imposed symmetry are the same.

Economic configurations based on $\mathcal{RT}_k$ spaces

Inspired by the $\mathscr{E}_{S-\mathcal{RT}_k}$ space configuration, the proposal in [12] is also to consider a formulation based on the Poisson-compatible $\mathcal{RT}_k$ space on simplicial elements, but augmented with divergence-free spaces of minimum dimension, while keeping the remaining configuration for displacement and rotation variables. A second version of this FE space configuration was proposed in [21], using a smaller stress space, displacement space with one degree less, while maintaining the same space for rotations.

6.3.2. Spaces based on $\mathcal{ABF}_{[k]}$ spaces, $k \geq 1$, for quadrilaterals

The $\mathcal{ABF}_{[k]}$ spaces were introduced in [5] for approximation of the Poisson problem on quadrilateral elements and correspond to $\hat{V}_{\mathcal{ABF}_{[k]}}(\hat{K},\mathbb{R}^2) = \mathbb{Q}_{k+2,k}(\hat{K},\mathbb{R}) \times \mathbb{Q}_{k,k+2}(\hat{K},\mathbb{R})$ and $\hat{P}_{\mathcal{ABF}_{[k]}}(\hat{K},\mathbb{R}) = R_k(\hat{K},\mathbb{R})$, where $R_k(\hat{K},\mathbb{R}) \subsetneq \mathbb{Q}_{k+1,k+1}(\hat{K},\mathbb{R})$ is obtained by excluding from the polynomials in $\mathbb{Q}_{k+1,k+1}(\hat{K},\mathbb{R})$ the span of the monomial $\hat{x}^{k+1}\hat{y}^{k+1}$. Accordingly, the associated local spaces are $V_{\mathcal{ABF}_{[k]}}(K,\mathbb{R}^2) = \mathbb{F}_K^{\mathrm{div}}(\hat{V}_{\mathcal{ABF}_{[k]}}(\hat{K},\mathbb{R}^2))$ and $P_{\mathcal{ABF}_{[k]}}(K,\mathbb{R}) = \mathbb{F}_K(\hat{P}_{\mathcal{ABF}_{[k]}}(\hat{K},\mathbb{R}))$. Based on the $\mathcal{ABF}_{[k]}$ family, the space configuration $\mathscr{E}_{\mathcal{ABF}_{[k]}} = \{\mathscr{S}_{\mathcal{ABF}_{[k]}}, \mathscr{U}_{\mathcal{ABF}_{[k]}}, \mathscr{Q}_{\mathcal{RT}_{[k]}}\}$,

studied in [26] is defined as follows:

$$\mathscr{S}_{\mathcal{ABF}_{[k]}} = \left\{ \underline{\underline{\tau}} \in H(\mathrm{div}, \Omega, \mathbb{M});\ \underline{\underline{\tau}}|_K \in S_{\mathcal{ABF}_{[k]}}(K, \mathbb{M}),\ K \in \mathcal{T} \right\},$$
$$\mathscr{U}_{\mathcal{ABF}_{[k]}} = \left\{ \underline{u} \in L^2(\Omega, \mathbb{R}^2);\ \underline{u}|_K \in U_{\mathcal{ABF}_{[k]}}(K, \mathbb{R}^2),\ K \in \mathcal{T} \right\},$$
$$\mathscr{Q}_{\mathcal{ABF}_{[k]}} = \mathscr{Q}_{\mathcal{RT}_{[k]}}.$$

Its stability is obtained after the observation that $V_{\mathcal{RT}_{[k]}}(K, \mathbb{R}^2) \subset V_{\mathcal{ABF}_{[k]}}(K, \mathbb{R}^2)$, and by using the same arguments for the verification of the hypotheses of Theorem 1, as done for $\mathscr{E}_{\mathcal{RT}_{[k]}}$ in [1] and described in Section 6.1.1.

As discussed in [18], the confrontation of the Poisson-compatible $\mathcal{ABF}_{[k]}$ and $\mathcal{RT}^+_{[k]}$ space configurations for quadrilateral elements reveals that their vector spaces in the master element share the same edge component, in $\mathbb{Q}_{k,k}(\hat{K}, \mathbb{R}^2)$, but $\mathring{V}_{\mathcal{ABF}_{[k]}} \subsetneq \mathring{V}_{\mathcal{RT}^+_{[k]}}$. Furthermore, $P_{\mathcal{ABF}_{[k]}}(\hat{K}, \mathbb{R}) \subsetneq \mathbb{Q}_{k+1,k+1}(\hat{K}, \mathbb{R}) = P_{\mathcal{RT}^+_{[k]}}(\hat{K}, \mathbb{R})$. Consequently, the convergence rates for $\mathscr{E}_{\mathcal{ABF}_{[k]}}$ and $\mathscr{E}_{\mathcal{RT}^+_{[k]}}$ are of the same order for $\underline{\underline{\sigma}}$ and $\underline{\nabla} \cdot \underline{\underline{\sigma}}$. Concerning their convergence rates for displacement, both reach the enhanced $k+2$ order for affine meshes, but for general quadrilaterals mapped by bilinear transformations the rate for $\mathscr{E}_{\mathcal{ABF}_{[k]}}$ spaces is of order $k+1$, while for $\mathscr{E}_{\mathcal{RT}^+_{[k]}}$ spaces the enhanced $k+2$ order is reached. For the approximation of the rotation the rate of convergence is $k+1$, for both schemes.

7. Numerical results

One possibility for the implementation of the method (6) in a reduced form is to apply static condensation. This procedure can be done after classifying, in each element, the degrees-of-freedom of the tensor unknowns as internal or edge shape functions, and of the displacement as piecewise constant approximations (rigid body motions) or functions with zero mean. Then the degrees-of-freedom associated with internal tensors, zero mean displacements and rotations can be condensed, leading to an indefinite linear system coupling the global unknowns of edge tensors and rigid body piecewise constant displacements.

An alternative implementation technique is via hybridization, as described, e.g., in [12], that results in a symmetric positive definite system for a single new variable. In the hybrid formulation, the $H(\mathrm{div}, \mathbb{M})$-conformity of the tensor approximation spaces $\mathscr{S}_h$ are relaxed, and a Lagrange multiplier, $\underline{\lambda}_h$, is introduced on the edges. This procedure allows for the condensation of all degrees-of-freedom associated with $\underline{\underline{\sigma}}_h$, $\underline{u}_h$, and q_h, resulting in a global system for $\underline{\lambda}_h$ only. The numerical results in this section have been obtained by the hybridization technique, using the general purpose MKL/Pardiso package to solve the global systems.

In order to illustrate the error analysis of the previous section, a test problem is defined in $\Omega = (0,1)^2$, and the load function $\underline{g}$ is chosen such that the model problem has exact solution given by

$$\underline{u}(x,y) = \begin{bmatrix} \cos(\pi x)\sin(2\pi y) \\ \sin(\pi x)\cos(\pi y) \end{bmatrix},$$

with the Lamé parameters $\lambda = 123$ and $\mu = 79.3$.

In the following sections we present numerical results that confirm the *a priori* error estimates obtained previously. For convenience, some of them are summarized in Table C.4, shall the reader reproduce these tests.

7.1. Uniform affine meshes

Uniform rectangular meshes are considered with spacing $h = 2^{-\ell}$, $\ell = 2, \ldots, 8$, and triangular meshes constructed from them by diagonal subdivision.

Rectangular elements

We show in Figure 1 the error curves for $\underline{\underline{\sigma}}$ (top left), for $\underline{\nabla} \cdot \underline{\underline{\sigma}}$ (bottom left), for $\underline{u}$ (top right), and for q (bottom right). The results are obtained with approximation space configurations $\mathscr{E}_{\mathcal{RT}_{[k]}}$, $\mathscr{E}_{\mathcal{RT}^{\sim}_{[k]}}$ and $\mathscr{E}_{\mathcal{RT}^{+}_{[k]}}$, for $k = 1$ and 2. For simplicity, these space configurations are indicated in the plots by $\mathcal{RT}_{[k]}$, $\mathcal{RT}^{\sim}_{[k]}$, and $\mathcal{RT}^{+}_{[k]}$, respectively. The expected rates of convergence are verified, illustrating the enhanced divergence and displacement accuracy when the enriched configurations are applied. In fact, confronted with $\mathscr{E}_{\mathcal{RT}_{[k]}}$ and $\mathscr{E}_{\mathcal{RT}^{\sim}_{[k]}}$, the configuration $\mathscr{E}_{\mathcal{RT}^{+}_{[k]}}$ gives approximations for the variables $\underline{\underline{\sigma}}$ and q with same accuracy order, h^{k+1}, but with smaller error magnitudes, specially for $k = 2$. Enhanced order h^{k+2} is verified for the variables $\underline{u}$ and $\underline{\nabla} \cdot \underline{\underline{\sigma}}$ when using the enriched configurations $\mathscr{E}_{\mathcal{RT}^{\sim}_{[k]}}$ and $\mathscr{E}_{\mathcal{RT}^{+}_{[k]}}$. The errors in tensor asymmetry are displayed in Figure 2. It can be observed that the convergence rates are of order h^{k+1}, which is consistent with the corresponding tensor accuracy. However, the use of enhanced rotation space in $\mathscr{E}_{\mathcal{RT}^{+}_{[k]}}$ results in an approximation for the stress tensor with reduced asymmetry.

Triangular elements

The plots in Figures 3 and 4 are for simulations based on triangular elements and the space configurations $\mathscr{E}_{\mathcal{BDM}_k}$ (indicated by $\mathcal{BDM}_k$), $\mathscr{E}_{\mathcal{BDM}^{+}_{k}}$ (indicated by $\mathcal{BDM}^{+}_{k}$), and $\mathscr{E}_{\mathcal{BDM}^{++}_{k}}$ (indicated by $\mathcal{BDM}^{++}_{k}$), for $k = 1$ and 2. In all cases, the convergence rates for the variables $\underline{\underline{\sigma}}$ and q are of order h^{k+1}. For $\underline{\nabla} \cdot \underline{\underline{\sigma}}$ and $\underline{u}$, the convergence rates increase from order h^{k}, when $\mathcal{BDM}_k$ is used, to orders h^{k+1} and h^{k+2}, when the space configurations are enriched to $\mathscr{E}_{\mathcal{BDM}^{+}_{k}}$ and $\mathscr{E}_{\mathcal{BDM}^{++}_{k}}$, respectively.

7.2. Trapezoidal meshes

The purpose of this test problem is to evaluate the effect on the accuracy of the approximation when non-affine quadrilateral meshes are used. Consider the partitions $\mathcal{T}_h$ of Ω formed by trapezoidal elements with a basis of length h and vertical parallel sides of lengths $0.75h$ and $1.25h$.

The error curves for $\underline{\underline{\sigma}}$, $\underline{\nabla} \cdot \underline{\underline{\sigma}}$, $\underline{u}$, and q are presented in Figures 5 and 6, using the approximation spaces of type $\mathscr{E}_{\mathcal{RT}_{[k]}}$, $\mathscr{E}_{\mathcal{RT}^{\sim}_{[k]}}$, and $\mathscr{E}_{\mathcal{RT}^{+}_{[k]}}$, for $k = 1$ and 2. As predicted by the estimates, the convergence rates for $\underline{\underline{\sigma}}$, $\underline{u}$, and q obtained with these non-affine trapezoidal meshes coincide with the ones obtained with uniform rectangular meshes, namely h^{k+1}, h^{k+2}, and h^{k+1}, respectively. For $\underline{\nabla} \cdot \underline{\underline{\sigma}}$, the degradation of accuracy to order h^{k} is verified for $\mathscr{E}_{\mathcal{RT}_{[k]}}$, but order h^{k+1} is recovered when the enriched space configurations $\mathscr{E}_{\mathcal{RT}^{\sim}_{[k]}}$ and $\mathscr{E}_{\mathcal{RT}^{+}_{[k]}}$ are applied.

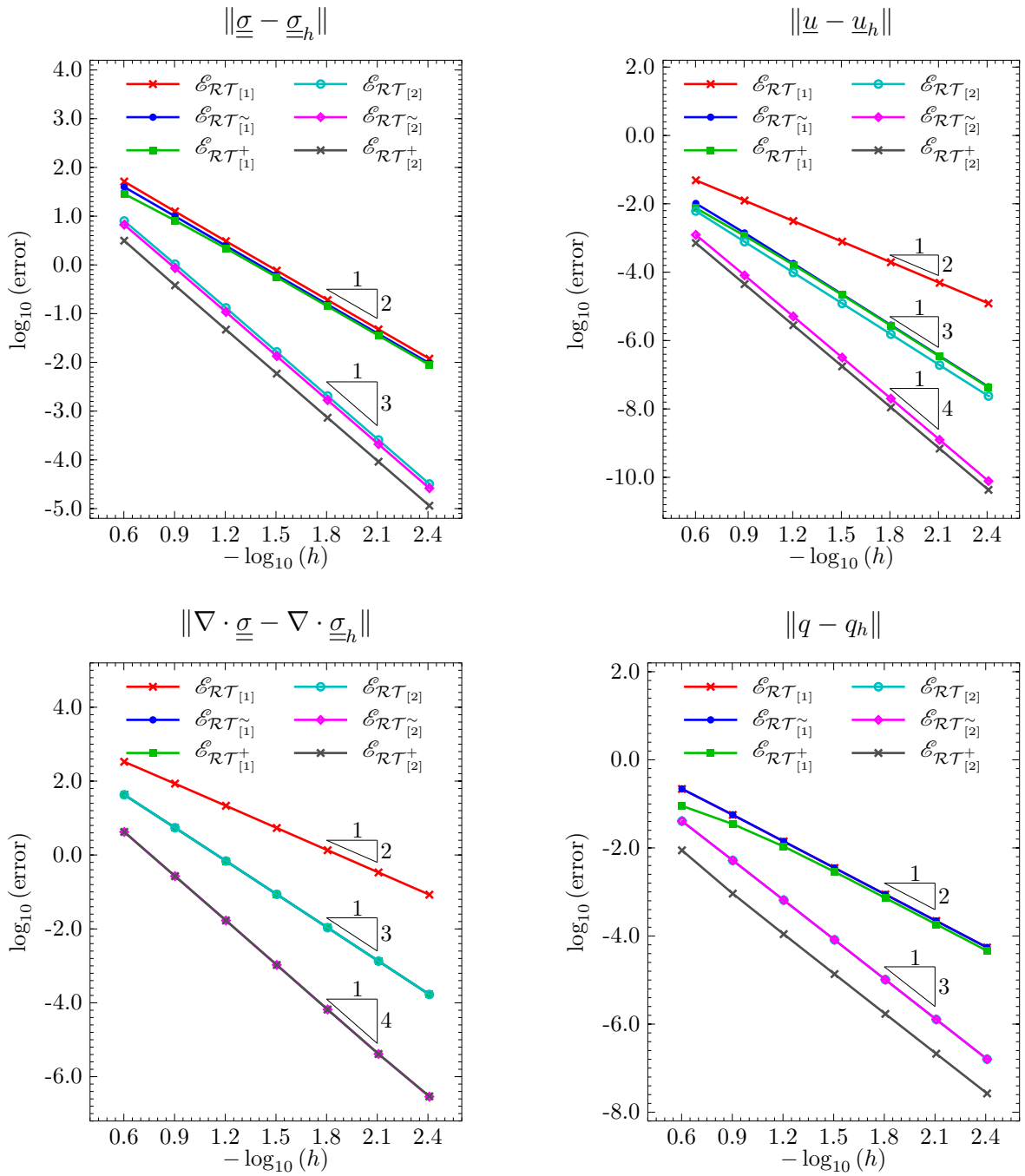

Figure 1: Rectangular meshes: L^2-error curves versus h for $\underline{\underline{\sigma}}$ (top left side), $\underline{u}$ (top right side), $\underline{\nabla} \cdot \underline{\underline{\sigma}}$ (bottom left side), and q (bottom right side), using space configurations $\mathscr{E}_{\mathcal{RT}_{[k]}}$, $\mathscr{E}_{\mathcal{RT}^{\sim}_{[k]}}$, and $\mathscr{E}_{\mathcal{RT}^{+}_{[k]}}$, for $k = 1$ and 2.

8. Conclusions

In this paper we demonstrate both theoretically and numerically that bubble enriched H(div) approximation spaces can be applied to the mixed formulation of two dimensional elasticity leading to higher rates of convergence for the divergence of the stress field and for the displacement. The compatibility between tensor and displacement spaces was inherited from previous work on the simulation of the Darcy problem [18]. It was also shown that the multiplier space for weakly enforcing the stress symmetry is Stokes-compatible with the enriched stress space.

The error analysis also demonstrates that weak stress symmetry enforcement and stress

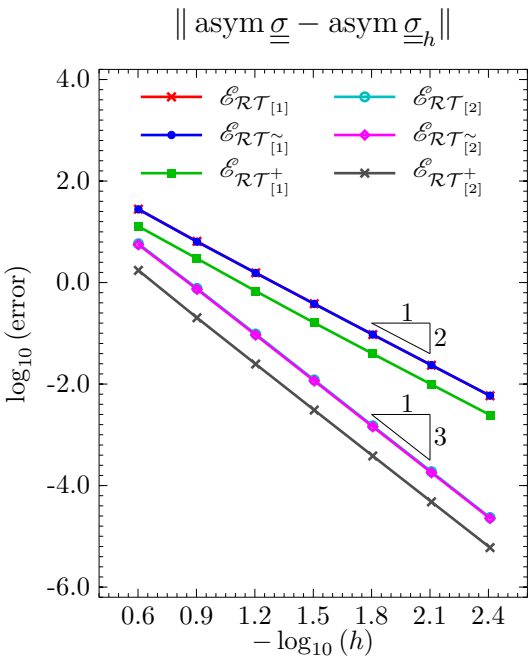

Figure 2: Rectangular meshes: L^2-error curves for $\operatorname{asym} \underline{\underline{\sigma}}$, using space configurations of type $\mathscr{E}_{\mathcal{RT}_{[k]}}$, $\mathscr{E}_{\mathcal{RT}^{\sim}_{[k]}}$, and $\mathscr{E}_{\mathcal{RT}^{+}_{[k]}}$, for $k = 1$ and 2.

accuracy are related. The proposed bubble enrichment has been used so that the convergence rate of the stress variable is determined by the order of approximation of the stress normal traces.

The additional degrees of freedom corresponding the the bubble degrees of freedom and higher order displacement space can be statically condensed. Therefore, the proposed approximation space leads to higher order accuracy for the displacements without affecting the size of the global system of equations.

The error estimates have been confirmed through numerical tests for both affine and distorted meshes, and for some some classic divergence compatible FE pairs.

As demonstrated in [15] for the case of Poisson-compatible FE pairs, the enrichment methodology is general enough to be considered for other elasticity families existing in the literature, provided their rotation multiplier space is Stokes-compatible with the enriched stress space.

Acknowledgments

The authors thankfully acknowledge financial support from CNPq – *Conselho Nacional de Desenvolvimento Científico e Tecnológico* (grants 305425/2013-7, and 304029/2013-0), and to FAPESP – *Fundação de Apoio à Pesquisa do Estado de São Paulo*, Brazil (grants 2016/05155, and 2017/08683-0). P. R. B. Devloo is grateful for the support and hospitality received during his visit to Beijing University of Technology, China, when part of this research has been performed.

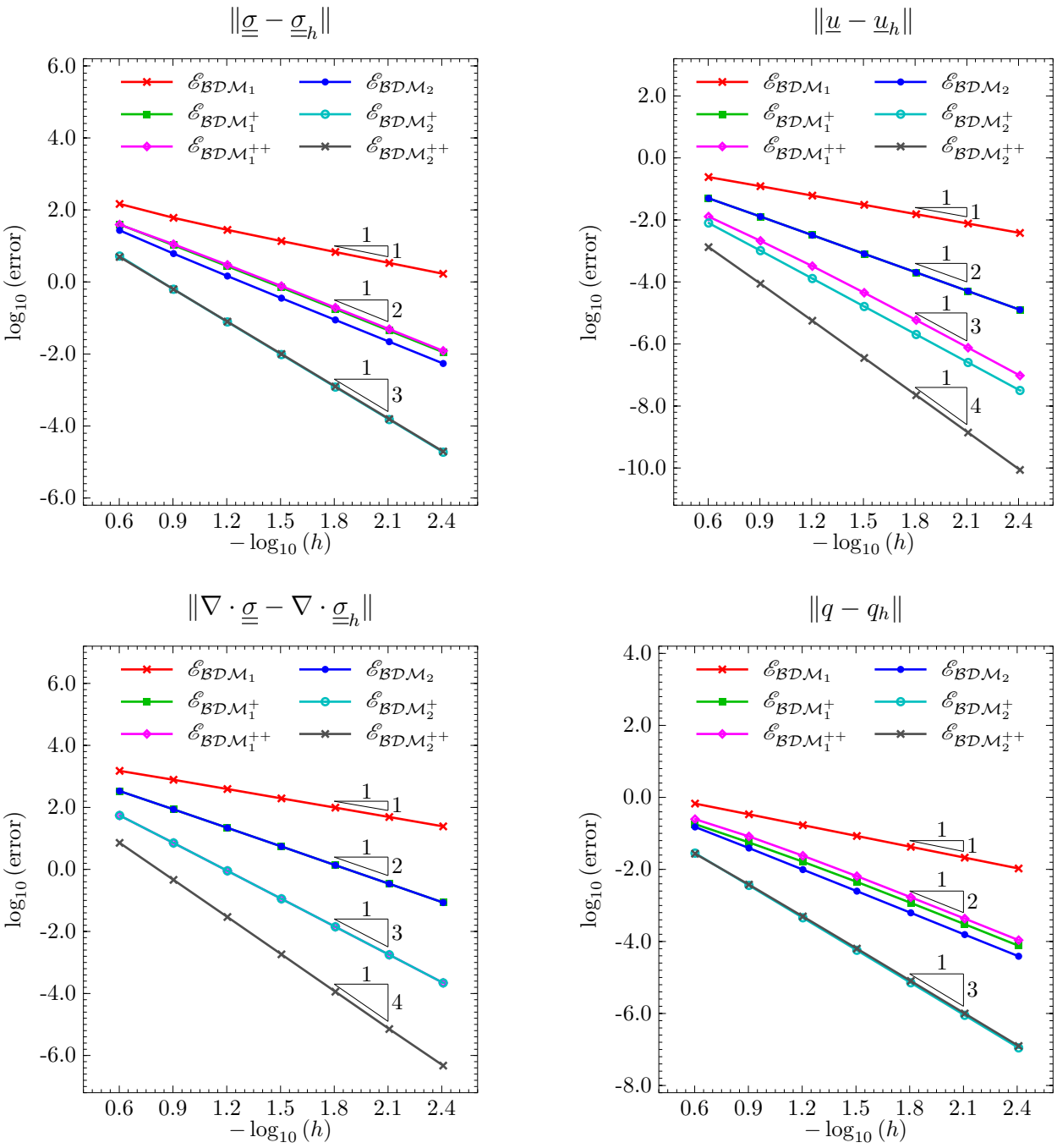

Figure 3: Triangular meshes: L^2-error curves versus h for $\underline{\underline{\sigma}}$ (top left side), $\underline{u}$ (top right side), $\underline{\nabla} \cdot \underline{\underline{\sigma}}$ (bottom left side), and q (bottom right side), using space configurations $\mathscr{E}_{\mathcal{BDM}_k}$, $\mathscr{E}_{\mathcal{BDM}_k^+}$, and $\mathscr{E}_{\mathcal{BDM}_k^{++}}$, for $k = 1$ and 2.

References

[1] D. N. Arnold, G. Awanou, and W. Qiu. Mixed finite elements for elasticity on quadrilateral meshes. *Adv. Comput. Math.*, 41(3):553–572, 2015.

[2] D. N. Arnold, G. Awanou, and R. Winther. Finite elements for symmetric tensors in three dimensions. *Math. Comp.*, 77(263):1229–1251, 2008.

[3] D. N. Arnold, G. Awanou, and R. Winther. Nonconforming tetrahedral mixed finite elements for elasticity. *Math. Models Methods Appl. Sci.*, 24(4):783–796, 2014.

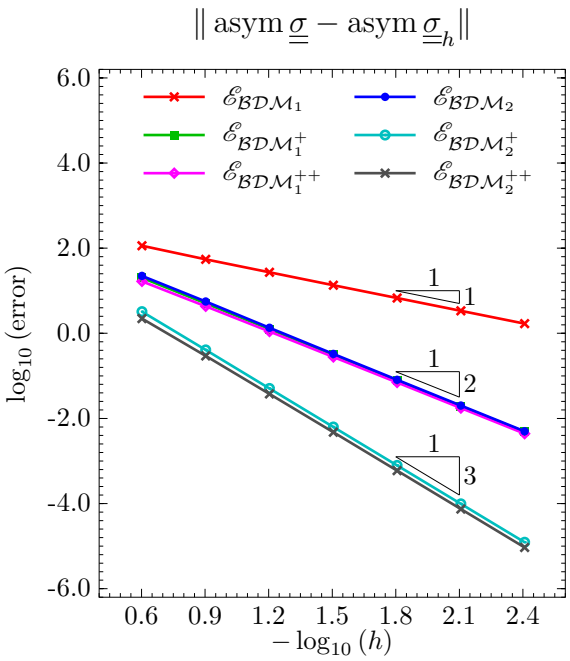

Figure 4: Triangular meshes: L^2-error curves versus h for $\operatorname{asym} \underline{\underline{\sigma}}$ using space configurations $\mathscr{E}_{\mathcal{BDM}_k}$, $\mathscr{E}_{\mathcal{BDM}_k^+}$, and $\mathscr{E}_{\mathcal{BDM}_k^{++}}$, for $k = 1$ and 2.

[4] D. N. Arnold, D. Boffi, and R. S. Falk. Approximation by quadrilateral finite elements. *Math. Comp.*, 71(239):909–922, 2002.

[5] D. N. Arnold, D. Boffi, and R. S. Falk. Quadrilateral $H(\mathrm{div})$ finite elements. *SIAM J. Numer. Anal.*, 42(6):2429–2451, 2005.

[6] D. N. Arnold, R. S. Falk, and R. Winther. Mixed finite element methods for linear elasticity with weakly imposed symmetry. *Math. Comp.*, 76(260):1699–1723, 2007.

[7] D. N. Arnold and R. Winther. Nonconforming mixed elements for elasticity. *Math. Models Methods Appl. Sci.*, 13(03):295–307, 2003.

[8] D. Boffi, F. Brezzi, and M. Fortin. Reduced symmetry elements in linear elasticity. *Commun. Pure Appl. Anal.*, 8(1):95–121, 2009.

[9] D. Boffi and L. Gastaldi. On the quadrilateral Q2-P1 element for the Stokes problem. *Int. J. Numer. Methods Fluids*, 39(11):1001–1011, 2002.

[10] F. Brezzi and M. Fortin. *Mixed and hybrid finite elements methods.* Springer Series in Computational Mathematics. Springer-Verlag, 1991.

[11] F. Brezzi and J. Pitkäranta. On the stabilization of finite element approximations of the Stokes equations. In W. Hackbusch, editor, *Efficient Solutions of Elliptic Systems: Proceedings of a GAMM-Seminar Kiel, January 27 to 29, 1984*, pages 11–19. Vieweg+Teubner Verlag, Wiesbaden, 1984.

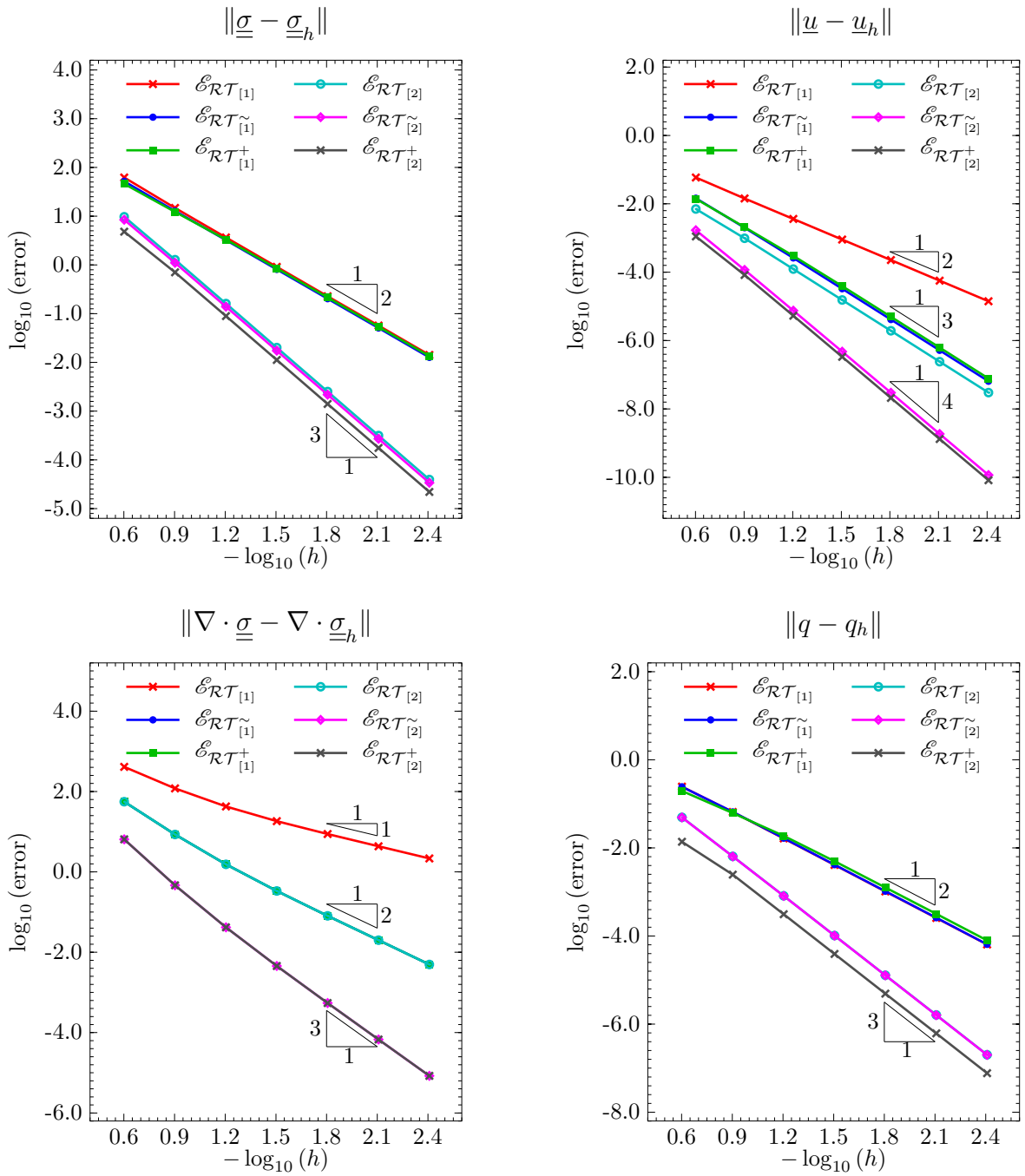

Figure 5: Trapezoidal meshes: L^2-error curves versus h for $\underline{\underline{\sigma}}$ (top left side), $\underline{u}$ (top right side), $\underline{\nabla} \cdot \underline{\underline{\sigma}}$ (bottom left side), and q (bottom right side), using space configurations $\mathscr{E}_{\mathcal{RT}_{[k]}}$, $\mathscr{E}_{\mathcal{RT}^{\sim}_{[k]}}$, and $\mathscr{E}_{\mathcal{RT}^{+}_{[k]}}$, for $k = 1$ and 2.

[12] B. Cockburn, J. Gopalakrishnan, and J. Guzmán. A new elasticity element made for enforcing weak stress symmetry. *Math. Comp.*, 79(271):1331–1349, 2010.

[13] M. Crouzeix and P. A. Raviart. Conforming and nonconforming finite element methods for solving the stationary Stokes equations I. *ESAIM Math. Model. Numer. Anal.*, 7(R3):33–75, 1973.

[14] P. R. B. Devloo, O. Durán, S. M. Gomes, and N. Shauer. Mixed finite element approx-

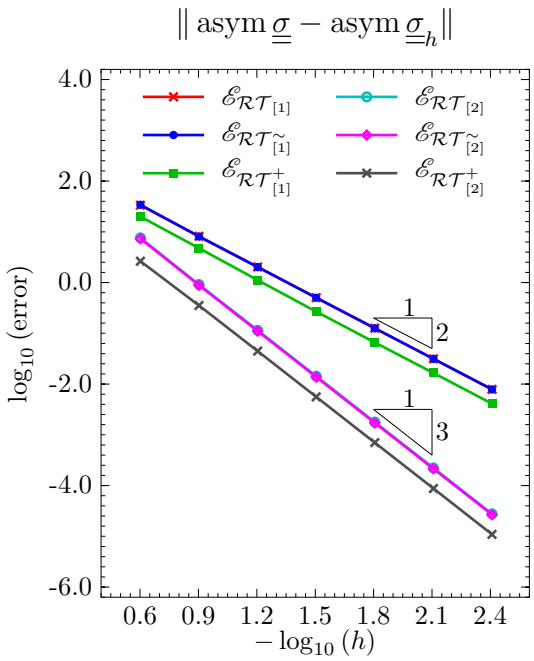

Figure 6: Trapezoidal meshes: L^2-error curves for $\operatorname{asym} \underline{\underline{\sigma}}$, using space configurations $\mathscr{E}_{\mathcal{RT}_{[k]}}$, $\mathscr{E}_{\mathcal{RT}^{\sim}_{[k]}}$, and $\mathscr{E}_{\mathcal{RT}^{+}_{[k]}}$, for $k = 1$ and 2.

imations based on 3-D hp-adaptive curved meshes with two types of H(div)-conforming spaces. *Int. J. Numer. Methods Engrg.*, 113(7):1045–1060, 2017.

[15] P. R. B. Devloo, A. M. Farias, and S. M. Gomes. A remark concerning divergence accuracy order for H(div)- conforming finite element flux approximations. *Comput. Math. with Appl.*, 77(7):1864–1872, 2019.

[16] R. S. Falk. Finite element methods for linear elasticity. In D. Boffi and L. Gastaldi, editors, *Mixed Finite Elements, Compatibility Conditions, and Applications*, volume 1939 of *Lecture Notes in Mathematics*, pages 159–194. Springer Berlin Heidelberg, 2008.

[17] M. Farhloul and M. Fortin. Dual hybrid methods for the elasticity and the Stokes problems: a unified approach. *Numer. Math.*, 76(4):419–440, 1997.

[18] A. M. Farias, P. R. B. Devloo, S. M. Gomes, D. de Siqueira, and D. A. Castro. Two dimensional mixed finite element approximations for elliptic problems with enhanced accuracy for the potential and flux divergence. *Comput. Math. with Appl.*, 74(12):3283–3295, 2017.

[19] B. M. Fraeijs de Veubeke. Stress function approach. In *Proc. of the World Congress on Finite Element Methods in Structural Mechanics*, volume 1, pages J.1–J.51. Bournemouth, Dorset, 1975.

[20] V. Girault and P. A. Raviart. *Finite element methods for Navier-Stokes equations: theory and algorithms*, volume 5 of *Springer Series in Computational Mathematics*. Springer-Verlag, 1986.

[21] J. Gopalakrishnan and J. Guzmán. A second elasticity element using the matrix bubble. *IMA J. Numer. Anal.*, 32(1):352–372, 2012.

[22] J. Hu, H. Man, and S.Y. Zhang. A simple conforming mixed finite element for linear elasticity on rectangular grids in any space dimension. *J. Sci. Comput.*, 58(2):367–379, 2014.

[23] H.-Y. Man, J. Hu, and Z.-C. Shi. Lower order rectangular nonconforming mixed finite element for the three-dimensional elasticity problem. *Math. Models Methods Appl. Sci.*, 19(01):51–65, 2009.

[24] L. Mansfield. Finite element subspaces with optimal rates of convergence for the stationary Stokes problem. *RAIRO Anal. Numer.*, 16(1):49–66, 1982.

[25] W. Qiu, J. Shen, and K. Shi. An HDG method for linear elasticity with strong symmetric stresses. *Math. Comput.*, 87(309):69–93, 2018.

[26] T. O. Quinelato, A. F. D. Loula, M. R. Correa, and T. Arbogast. Full H(div)-approximation of linear elasticity on quadrilateral meshes based on ABF finite elements. *Comput. Methods in Appl. Mech. Eng.*, 347:120–142, 2019.

[27] R. Stenberg. On the construction of optimal mixed finite element methods for the linear elasticity problem. *Numer. Math.*, 48(4):447–462, 1986.

[28] R. Stenberg. A family of mixed finite elements for the elasticity problem. *Numer. Math.*, 53(5):513–538, 1988.

[29] R. Stenberg and M. Suri. Mixed hp finite element methods for problems in elasticity and Stokes flow. *Numer. Math.*, 72(3):367–389, 1996.

[30] S.-Y. Yi. Nonconforming mixed finite element methods for linear elasticity using rectangular elements in two and three dimensions. *Calcolo*, 42(2):115–133, 2005.

Appendix A. Proof of Theorem 2

Proof. The construction of $\boldsymbol{\Pi}\underline{\underline{\tau}} = \boldsymbol{\Pi}_1\underline{\underline{\tau}} + \boldsymbol{\Pi}_2\underline{\underline{\tau}}$ is done in two steps. First, choose $\boldsymbol{\Pi}_1 : H^{s+1}(\Omega, \mathbb{M}) \to \mathscr{S}$ such that

$$\left(\underline{\nabla} \cdot (\underline{\underline{\tau}} - \boldsymbol{\Pi}_1\underline{\underline{\tau}}), \underline{\eta}\right), = 0, \ \forall \underline{\eta} \in \mathscr{U}. \tag{A.1}$$

This can be obtained directly from the projection associated to the pair $\{\mathscr{V}, \mathscr{P}\}$, $\boldsymbol{\pi}^D : H^s(\Omega, \mathbb{R}^2) \to \mathscr{V}$, verifying the commutation formula (4b). Precisely, for $\underline{\underline{\tau}} = \begin{bmatrix} \underline{\psi_1} & \underline{\psi_2} \end{bmatrix} \in \mathscr{S}$, let $\boldsymbol{\Pi}_1\underline{\underline{\tau}} =$

$\left[\boldsymbol{\pi}^D\underline{\psi_1} \quad \boldsymbol{\pi}^D\underline{\psi_2}\right]$. Then $\boldsymbol{\Pi}_1$ is a bounded operator in $H(\mathrm{div},\Omega,\mathbb{M})$, and

$$\begin{aligned}\left(\underline{\nabla}\cdot(\underline{\underline{\tau}}-\boldsymbol{\Pi}_1\underline{\underline{\tau}}),\underline{\eta}\right) &= \left[\left(\nabla\cdot(\psi_1-\boldsymbol{\pi}^D\psi_1),\eta_1\right),\left(\nabla\cdot(\psi_2-\boldsymbol{\pi}^D\psi_2),\eta_2\right)\right]\\ &= 0,\ \forall\underline{\eta}=\left[\eta_1 \quad \eta_2\right]\in\mathscr{U}.\end{aligned}$$

The second step is a divergence free correction $\boldsymbol{\Pi}_2 : H^{s+1}(\Omega,\mathbb{M})\to\mathscr{S}$ such that

$$(\text{asym }\boldsymbol{\Pi}_2\underline{\underline{\tau}},\varphi) = (\text{asym }(\boldsymbol{\Pi}_1\underline{\underline{\tau}}-\underline{\underline{\tau}}),\varphi),\ \forall\varphi\in\mathscr{Q}. \tag{A.2}$$

To construct $\boldsymbol{\Pi}_2\underline{\underline{\tau}}$, let $\underline{\phi}=[\phi_1\ \phi_2]\in\mathscr{W}$ be a solution of the Stokes problem such that $-(\nabla\cdot\underline{\phi},\varphi)=(\mathrm{asym}(\boldsymbol{\Pi}_1\underline{\underline{\tau}}-\underline{\underline{\tau}}),\varphi),\ \forall\varphi\in\mathscr{Q}$, and define

$$\boldsymbol{\Pi}_2\underline{\underline{\tau}} = \underline{\underline{\nabla}}\times\underline{\phi} = \begin{bmatrix}\partial_2\phi_1 & -\partial_1\phi_1\\ \partial_2\phi_2 & -\partial_1\phi_2\end{bmatrix}.$$

By the assumption of Theorem 1, $\boldsymbol{\Pi}_2\underline{\underline{\tau}}\in\mathscr{S}$. It can be easily verified that $\boldsymbol{\Pi}_2\underline{\underline{\tau}}$ is divergence free. Consequently,

$$\|\boldsymbol{\Pi}_2\underline{\underline{\tau}}\|_{H(\mathrm{div},\Omega,\mathbb{M})} = \|\boldsymbol{\Pi}_2\underline{\underline{\tau}}\|_{L^2(\Omega,\mathbb{M})} \le C\|\boldsymbol{\Pi}_1\underline{\underline{\tau}}-\underline{\underline{\tau}}\|_{L^2(\Omega,\mathbb{M})},$$

and since asym $\boldsymbol{\Pi}_2\underline{\underline{\tau}} = -\partial_1\phi_1-\partial_2\phi_2 = -\nabla\cdot\underline{\phi}$, the required property (A.2) holds. □

Appendix B. Proof of Theorem 3

Proof. The proof is obtained with similar arguments as in Theorem 6.1 in [5]. Consider the errors $\underline{\underline{\sigma}}-\underline{\underline{\sigma}}_h$, $\underline{u}-\underline{u}_h$ and $q-q_h$. Then

$$(\mathbf{A}(\underline{\underline{\sigma}}-\underline{\underline{\sigma}}_h),\underline{\underline{\tau}}) + (\underline{u}-\underline{u}_h,\underline{\nabla}\cdot\underline{\underline{\tau}}) + (q-q_h,\text{asym }\underline{\underline{\tau}}) = 0, \quad \forall\underline{\underline{\tau}}\in\mathscr{S}_h, \tag{B.1}$$

$$(\underline{\nabla}\cdot(\underline{\underline{\sigma}}-\underline{\underline{\sigma}}_h),\underline{\eta}) = 0, \quad \forall\underline{\eta}\in\mathscr{U}_h, \tag{B.2}$$

$$(\mathrm{asym}(\underline{\underline{\sigma}}-\underline{\underline{\sigma}}_h),\varphi) = 0, \quad \forall\varphi\in\mathscr{Q}_h. \tag{B.3}$$

Taking $\underline{\underline{\tau}}=\boldsymbol{\Pi}_h\underline{\underline{\sigma}}-\underline{\underline{\sigma}}_h\in\mathscr{S}_h$, and using equation (B.2), combined with properties (11) and (15), we obtain

$$\begin{aligned}(\underline{u}-\underline{u}_h,\underline{\nabla}\cdot\underline{\underline{\tau}}) &= (\Lambda_h\underline{u}-\underline{u}_h,\underline{\nabla}\cdot(\boldsymbol{\Pi}_h\underline{\underline{\sigma}}-\underline{\underline{\sigma}}_h))\\ &= (\Lambda_h\underline{u}-\underline{u}_h,\underline{\nabla}\cdot(\underline{\underline{\sigma}}-\underline{\underline{\sigma}}_h)) = 0.\end{aligned} \tag{B.4}$$

Analogously, from equation (B.3), combined with (11), we obtain

$$0 = \Big(\text{asym}(\underline{\underline{\sigma}} - \boldsymbol{\Pi}_h\underline{\underline{\sigma}} + \boldsymbol{\Pi}_h\underline{\underline{\sigma}} - \underline{\underline{\sigma}}_h), \varphi\Big) = \Big(\text{asym}(\underline{\underline{\sigma}} - \boldsymbol{\Pi}_h\underline{\underline{\sigma}}), \varphi\Big) + \Big(\text{asym}\,\underline{\underline{\tau}}, \varphi\Big)$$
$$= \Big(\text{asym}\,\underline{\underline{\tau}}, \varphi\Big)\,,\ \forall \varphi \in \mathscr{Q}_h. \tag{B.5}$$

Consequently, by using $\underline{\underline{\tau}} = \boldsymbol{\Pi}_h\underline{\underline{\sigma}} - \underline{\underline{\sigma}}_h$ as test function in (B.1), we obtain $(\mathbf{A}(\underline{\underline{\sigma}} - \underline{\underline{\sigma}}_h), \underline{\underline{\tau}}) + (q - \Gamma_h q, \text{asym}\,\underline{\underline{\tau}}) = 0$, which can be expressed as

$$(\mathbf{A}(\underline{\underline{\sigma}} - \boldsymbol{\Pi}_h\underline{\underline{\sigma}} + \boldsymbol{\Pi}_h\underline{\underline{\sigma}} - \underline{\underline{\sigma}}_h), \underline{\underline{\tau}}) + (q - \Gamma_h q, \text{asym}\ \underline{\underline{\tau}}) = 0,$$

meaning that

$$(\mathbf{A}(\boldsymbol{\Pi}_h\underline{\underline{\sigma}} - \underline{\underline{\sigma}}), \underline{\underline{\tau}}) + (\Gamma_h q - q,\ \text{asym}\ \underline{\underline{\tau}}) = (\mathbf{A}\underline{\underline{\tau}}, \underline{\underline{\tau}}).$$

Using (B.4) and (B.5), the condition (S1) implies that $(\mathbf{A}\underline{\underline{\tau}}, \underline{\underline{\tau}}) \geq c_1^{-2}\|\underline{\underline{\tau}}\|^2_{H(\text{div},\Omega,\mathbb{M})} = c_1^{-2}\|\underline{\underline{\tau}}\|^2_{L^2(\Omega,\mathbb{M})}$.

Consequently,

$$\|\underline{\underline{\tau}}\|_{L^2(\Omega,\mathbb{M})} = \|\boldsymbol{\Pi}_h\underline{\underline{\sigma}} - \underline{\underline{\sigma}}_h\|_{L^2(\Omega,\mathbb{M})} \leq C\left[\|\boldsymbol{\Pi}_h\underline{\underline{\sigma}} - \underline{\underline{\sigma}}\|_{L^2(\Omega,\mathbb{M})} + \|\Gamma_h q - q\|_{L^2(\Omega,\mathbb{R})}\right], \tag{B.6}$$

holds. The above relation is the statement of Theorem 4.1 in [12], derived in the context of simplex meshes.

Concerning the estimate for $\|q - q_h\|_{L^2(\Omega,\mathbb{R})}$, let $\underline{\phi}_h \in \mathscr{W}_h$ be an approximation of a vector function $\underline{\phi} \in H^1(\Omega, \mathbb{R}^2)$, with $-\nabla\cdot\underline{\phi} = \Gamma_h q - q_h$, by the mixed formulation of a Stokes problem based on the space configuration $\{\mathscr{W}_h,\ \mathscr{Q}_h\}$ such that $-(\nabla\cdot\underline{\phi}_h, \varphi) = (\Gamma_h q - q_h, \varphi),\ \forall\varphi \in \mathscr{Q}_h$. Defining $\underline{\underline{\tau}} = \underline{\underline{\nabla}} \times \underline{\phi}_h \in \mathscr{S}_h$, then $\underline{\nabla}\cdot\underline{\underline{\tau}} = \underline{0}$, and $\text{asym}\,\underline{\underline{\tau}} = -\nabla\cdot\underline{\phi}_h$. Thus, $\|\Gamma_h q - q_h\|^2_{L^2(\Omega,\mathbb{R})} = -(\nabla\cdot\underline{\phi}_h, \Gamma_h q - q_h)$. Using this expression in the error relation (B.1), we get

$$-(\mathbf{A}(\underline{\underline{\sigma}} - \underline{\underline{\sigma}}_h), \underline{\underline{\tau}}) - (q - \Gamma_h q, \text{asym}\ \underline{\underline{\tau}}) = \|\Gamma_h q - q_h\|^2_{L^2(\Omega,\mathbb{R})}$$

from which the estimate

$$\|\Gamma_h q - q_h\|_{L^2(\Omega,\mathbb{R})} \leq C\left[\|\underline{\underline{\sigma}} - \underline{\underline{\sigma}}_h\|_{L^2(\Omega,\mathbb{M})} + \|q - \Gamma_h q\|_{L^2(\Omega,\mathbb{R})}\right] \tag{B.7}$$

holds. Similar result is stated in [12, Theorem 6.1]. Combining (B.7) with the (B.6), the desired estimate (B.1) is derived after the application of the triangle inequality.

In the case of affine meshes, for which $\underline{\nabla}\cdot\underline{\underline{\sigma}}_h \in \mathscr{U}_h$, (B.2) means that $\underline{\nabla}\cdot\underline{\underline{\sigma}}_h$ is the L^2-projection of $\underline{\nabla}\cdot\underline{\underline{\sigma}}$ on $\mathscr{U}_h$. Consequently, estimates (22) hold with $C = 1$. In general, in order to estimate the divergence error, a procedure similar to the one applied for the Poisson problem in [5, Theorem 6.1] may be used. Precisely, if $\underline{\underline{\tau}} \in \mathscr{S}_h$, define $\underline{\eta} \in \mathscr{U}_h$ by

$$\underline{\eta} = \begin{cases} \mathbf{J}_K\underline{\nabla}\cdot\underline{\underline{\tau}}, & \text{in } K \\ 0 & \text{elsewhere} \end{cases}$$

For the particular case $\underline{\underline{\tau}} = \underline{\underline{\sigma}}_h$, insert the result in (B.2) to get

$$(\underline{\nabla} \cdot (\underline{\underline{\sigma}} - \underline{\underline{\sigma}}_h), \mathbf{J}_K \underline{\nabla} \cdot \underline{\underline{\sigma}}_h) = 0,$$

from which the relation

$$\|\mathbf{J}_K^{1/2} \underline{\nabla} \cdot \underline{\underline{\sigma}}_h\|_{L^2(K,\mathbb{R}^2)} \leq \|\mathbf{J}_K^{1/2} \underline{\nabla} \cdot \underline{\underline{\sigma}}\|_{L^2(K,\mathbb{R}^2)},$$

holds, so $\|\underline{\nabla} \cdot \underline{\underline{\sigma}}_h\|_{L^2(K,\mathbb{R}^2)} \leq C \|\underline{\nabla} \cdot \underline{\underline{\sigma}}\|_{L^2(K,\mathbb{R}^2)}$. Similarly, taking $\underline{\eta}$ associated to $\underline{\underline{\tau}} = \boldsymbol{\Pi}_h \underline{\underline{\sigma}} - \underline{\underline{\sigma}}_h$, the relation

$$(\underline{\nabla} \cdot (\underline{\underline{\sigma}} - \underline{\underline{\sigma}}_h), \mathbf{J}_K \nabla \cdot (\boldsymbol{\Pi}_h \underline{\underline{\sigma}} - \underline{\underline{\sigma}}_h)) = 0$$

holds, from which we get

$$\|\underline{\nabla} \cdot (\underline{\underline{\sigma}} - \underline{\underline{\sigma}}_h)\|_{L^2(K,\mathbb{R}^2)} \leq C \|\underline{\nabla} \cdot (\boldsymbol{\Pi}_h \underline{\underline{\sigma}} - \underline{\underline{\sigma}})\|_{L^2(K,\mathbb{R}^2)}.$$

The estimate (22) follows by summing these contributions over all elements K.

In order to treat $\|\Lambda_h \underline{u} - \underline{u}_h\|^2_{L^2(\Omega,\mathbb{R}^2)}$, take $\underline{w}$ as the solution of the elasticity problem $\nabla \cdot \underline{\underline{v}} = \Lambda_h \underline{u} - \underline{u}_h$, with $\underline{\underline{v}} = \mathbf{A}^{-1} \boldsymbol{\epsilon} \underline{w} \in H(\mathrm{div}, \Omega, \mathbb{S})$, $\underline{w}|_{\partial\Omega} = 0$. Therefore,

$$\begin{aligned}
\|\Lambda_h \underline{u} - \underline{u}_h\|^2_{L^2(\Omega,\mathbb{R}^2)} &= (\underline{\nabla} \cdot \underline{\underline{v}}, \Lambda_h \underline{u} - \underline{u}_h) = (\underline{\nabla} \cdot \boldsymbol{\Pi}_h \underline{\underline{v}}, \Lambda_h \underline{u} - \underline{u}_h) \qquad \text{(by (11))} \\
&= (\underline{\nabla} \cdot \boldsymbol{\Pi}_h \underline{\underline{v}}, \underline{u} - \underline{u}_h) + (\underline{\nabla} \cdot \boldsymbol{\Pi}_h \underline{\underline{v}}, \Lambda_h \underline{u} - \underline{u}) \\
&= (\underline{\nabla} \cdot \boldsymbol{\Pi}_h \underline{\underline{v}}, \underline{u} - \underline{u}_h) \qquad \text{(by (15))}. \qquad \text{(B.8)}
\end{aligned}$$

Since $\underline{\underline{v}}$ is a symmetric tensor, and $\Big(\mathrm{asym}(\underline{\underline{v}} - \boldsymbol{\Pi}_h \underline{\underline{v}}), \varphi\Big) = 0, \ \forall \ \varphi \in \mathscr{Q}$, by property (11) we obtain that $(\mathrm{asym}\ (\boldsymbol{\Pi}_h \underline{\underline{v}}), \varphi) = 0, \ \forall \ \varphi \in \mathscr{Q}_h$, implying that

$$(q - q_h, \mathrm{asym}\ \boldsymbol{\Pi}_h \underline{\underline{v}}) = (q - \Gamma_h q, \mathrm{asym}\ (\underline{\underline{v}} - \boldsymbol{\Pi}_h \underline{\underline{v}})).$$

Noting that

$$\begin{aligned}
(\mathbf{A}(\underline{\underline{\sigma}} - \underline{\underline{\sigma}}_h), \underline{\underline{v}}) &= ((\underline{\underline{\sigma}} - \underline{\underline{\sigma}}_h), \boldsymbol{\epsilon} \underline{w}) = -(\underline{\nabla} \cdot (\underline{\underline{\sigma}} - \underline{\underline{\sigma}}_h), \underline{w}) \\
&= -(\underline{\nabla} \cdot (\underline{\underline{\sigma}} - \underline{\underline{\sigma}}_h), \underline{w} - \Lambda_h \underline{w}) = 0, \qquad \text{(by (15))},
\end{aligned}$$

we conclude that

$$\begin{aligned}
(\mathbf{A}(\underline{\underline{\sigma}} - \underline{\underline{\sigma}}_h), \boldsymbol{\Pi}_h \underline{\underline{v}}) &= -(\mathbf{A}(\underline{\underline{\sigma}} - \underline{\underline{\sigma}}_h), \underline{\underline{v}} - \boldsymbol{\Pi}_h \underline{\underline{v}}) + (\mathbf{A}(\underline{\underline{\sigma}} - \underline{\underline{\sigma}}_h), \underline{\underline{v}}) \\
&= -(\mathbf{A}(\underline{\underline{\sigma}} - \underline{\underline{\sigma}}_h), \underline{\underline{v}} - \boldsymbol{\Pi}_h \underline{\underline{v}}).
\end{aligned}$$

Then, after testing (B.1) with $\boldsymbol{\Pi}_h \underline{\underline{v}}$, we obtain the identity

$$(\mathbf{A}(\underline{\underline{\sigma}} - \underline{\underline{\sigma}}_h), \boldsymbol{\Pi}_h \underline{\underline{v}}) + (\underline{u} - \underline{u}_h, \underline{\nabla} \cdot \boldsymbol{\Pi}_h \underline{\underline{v}}) + (q - \Gamma_h q, \mathrm{asym}\ (\underline{\underline{v}} - \boldsymbol{\Pi}_h \underline{\underline{v}})) = 0,$$

to finally reach the desired relation after using (B.8):

$$\|\Lambda_h \underline{u} - \underline{u}_h\|^2_{L^2(\Omega,\mathbb{R}^2)} = (\mathbf{A}(\underline{\underline{\sigma}} - \underline{\underline{\sigma}}_h), \underline{\underline{v}} - \mathbf{\Pi}_h \underline{\underline{v}}) + (\Gamma_h q - q, \text{asym}\,(\underline{\underline{v}} - \mathbf{\Pi}_h \underline{\underline{v}})).$$

Recall that this result is related to [12, Theorem 5.1]. □

Appendix C. Table of convergence history

Rectangular elements

$\mathscr{E}_{\mathcal{RT}^+_{[2]}}$

ℓ	stress		displacement		divergence		rotation		asymmetry	
	error	rate	error	rate	error	rate	error	rate	error	rate
3	3.7966e−1	3.05	4.4881e−5	3.98	2.6844e−1	3.97	9.1537e−4	3.27	2.0264e−1	3.10
4	4.7075e−2	3.01	2.8192e−6	3.99	1.6856e−2	3.99	1.1013e−4	3.06	2.4738e−2	3.03
5	5.8717e−3	3.00	1.7644e−7	4.00	1.0547e−3	4.00	1.3656e−5	3.01	3.0708e−3	3.01
6	7.3349e−4	3.00	1.1031e−8	4.00	6.5939e−5	4.00	1.7041e−6	3.00	3.8303e−4	3.00
7	9.1666e−5	3.00	6.8946e−10	4.00	4.1216e−6	4.00	2.1294e−7	3.00	4.7843e−5	3.00

Trapezoidal elements

$\mathscr{E}_{\mathcal{RT}^+_{[2]}}$

ℓ	stress		displacement		divergence		rotation		asymmetry	
	error	rate	error	rate	error	rate	error	rate	error	rate
3	7.0365e−1	2.77	8.2708e−5	3.75	4.6390e−1	3.79	2.4684e−3	2.48	3.5236e−1	2.90
4	8.9174e−2	2.98	5.3090e−6	3.96	4.1611e−2	3.48	3.1180e−4	2.98	4.4620e−2	2.98
5	1.1206e−2	2.99	3.3516e−7	3.99	4.5372e−3	3.20	3.9194e−5	2.99	5.5938e−3	3.00
6	1.4038e−3	3.00	2.1028e−8	3.99	5.4433e−4	3.06	4.9126e−6	3.00	6.9961e−4	3.00
7	1.7564e−4	3.00	1.3163e−9	4.00	6.7309e−5	3.02	6.1488e−7	3.00	8.7455e−5	3.00

Triangular elements

$\mathscr{E}_{\mathcal{BDM}^+_2}$

ℓ	stress		displacement		divergence		rotation		asymmetry	
	error	rate	error	rate	error	rate	error	rate	error	rate
3	6.3008e−1	3.06	1.0249e−3	2.96	7.1264e+0	2.95	3.6031e−3	2.98	4.0618e−1	2.99
4	7.7523e−2	3.02	1.2911e−4	2.99	8.9841e−1	2.99	4.5303e−4	2.99	5.0600e−2	3.00
5	9.6450e−3	3.01	1.6171e−5	3.00	1.1254e−1	3.00	5.6752e−5	3.00	6.3112e−3	3.00
6	1.2040e−3	3.00	2.0223e−6	3.00	1.4075e−2	3.00	7.0998e−6	3.00	7.8799e−4	3.00
7	1.5044e−4	3.00	2.5282e−7	3.00	1.7596e−3	3.00	8.8777e−7	3.00	9.8441e−5	3.00

$\mathscr{E}_{\mathcal{BDM}^{++}_2}$

ℓ	stress		displacement		divergence		rotation		asymmetry	
	error	rate	error	rate	error	rate	error	rate	error	rate
3	6.2866e−1	2.97	8.7851e−5	3.92	4.6248e−1	3.95	3.7916e−3	2.85	2.9433e−1	2.91
4	7.9252e−2	2.99	5.6127e−6	3.97	2.9133e−2	3.99	4.9671e−4	2.93	3.7636e−2	2.97
5	9.9507e−3	2.99	3.5414e−7	3.99	1.8244e−3	4.00	6.3334e−5	2.97	4.7403e−3	2.99
6	1.2467e−3	3.00	2.2231e−8	3.99	1.1408e−4	4.00	7.9864e−6	2.99	5.9411e−4	3.00
7	1.5602e−4	3.00	1.3923e−9	4.00	7.1311e−6	4.00	1.0024e−6	2.99	7.4340e−5	3.00

Table C.4: L^2-errors and orders of convergence in the stress ($\underline{\underline{\sigma}}$), displacement ($\underline{u}$), divergence of stress ($\nabla \cdot \underline{\underline{\sigma}}$), rotation ($q$), and asymmetry of stress (asym $\underline{\underline{\sigma}}$), using approximation space configurations $\mathscr{E}_{\mathcal{RT}^+_{[2]}}$ on rectangular and trapezoidal meshes, and $\mathscr{E}_{\mathcal{BDM}^+_2}$ and $\mathscr{E}_{\mathcal{BDM}^{++}_2}$ on triangles.